Engine Concept for Operating on Fuel Gas - Sisu Diesel 420 DWRIE

Gerard Benseny Ràfales

Guillem Prats Teixido

Bachelor Thesis for Bachelor of Engineering

Degree Programme in Energy Technology

Vaasa, Finland, 2021

ACKNOWLEDGEMENTS

We would like to thank our esteemed supervisors Philip Hollins and Leif Backlund for their continuous help and advice during this thesis. Their knowledge and constant feedback steered us through this research. Our gratitude extends to Kaj Rintanen and the Novia University of Applied Science for their support in providing us with the required tools to conduct this thesis. Finally, we would also like to express gratitude to the companies AGCO Power Inc and Sandfirden Technics, for their support in providing technical documentation.

DEGREE THESIS

Author: Gerard Benseny Ràfales & Guillem Prats Teixido

Degree Programme: Mechanical Engineering

Specialization: Energy Technology

Supervisors: Philip Hollins and Leif Backlund

Title: Engine Concept for Operating on Fuel Gas

Date	Number of pages	Appendices
14.05.2021	71	4

Abstract

Alternative fuels for internal combustion engines, such as fuel gases, are a transition solution that could be beneficial in reducing current engine emissions before the electric vehicle becomes widespread. This thesis aimed to define the engine concept for converting an existing diesel engine (Sisudiesel 420 DWRIE) in the Novia University of Applied Science (Vaasa, Finland) laboratory, to a dedicated fuel gas engine, which will be used for academic and research purposes.

The thesis reviewed a range of available fuel gases and explored the possibilities for converting the diesel engine to operate on the selected fuel gas, defining a feasible engine concept. The resulting engine was simulated with GT-Power software to check its operation and performance.

As a result, it was found that Compressed Natural Gas was the most appropriate fuel for being implemented, according to engine conversion feasibility, fuel availability, and storage ease. Regarding the gas engine concept, it was determined to adopt a spark-ignition engine with a Venturi air-gas mixer and a reduced compression ratio compared to the original engine. The simulation results showed a consistent engine although there was a decrease in performance compared to the diesel engine. The findings of the thesis can provide a basis for future research in terms of engine optimization and engine concept physical implementation.

Language: English

Keywords: Fuel Gas, CNG, Diesel Engine, GT-Power, Sisudiesel, Natural Gas

TABLE OF CONTENTS

1. Introduction....1
2. Aims and objectives....3
3. Review of literature....4
3.1. Sisudiesel 420 DWRIE engine....4
3.1.1. AGCO Power Inc.....4
3.1.2. Sisudiesel 420 DWRIE specifications....5
3.1.3. Diesel....7
3.2. Review of available fuel gases....8
3.2.1. Main characteristics of fuel gases....8
3.2.1.1. Biogas....9
3.2.1.2. Natural gas and biomethane....9
3.2.1.3. Liquefied Petroleum Gas....10
3.2.2. Fuel availability....11
3.2.3. Fuel gas selection....12
3.2.4. Compressed Natural Gas....13
3.3. Engine modifications to operate on natural gas....17
3.3.1. Natural gas engine requirements....17
3.3.2. Possible diesel engine modifications to operate on natural gas....18
3.3.2.1. Ignition system....18
3.3.2.2. Compression ratio reduction....18
3.3.2.3. Fuel supply and mixing system....20
3.4. SGI-4 industrial gas engine – a case study....21
4. Natural gas engine concept....23
4.1. Proposed strategies and concepts....23
4.1.1. Concept 1. SI engine with DI and the existing cylinder head....24
4.1.2. Concept 2. SI engine with DI and replaced cylinder head....26
4.1.3. Concept 3. SI engine with mixing device....27
4.2. Selected engine concept....29

4.2.1. Ignition system 30
4.2.2. Compression ratio reduction 31
4.2.3. Fuel supply and mixing system 33
5. Engine modelling 36
5.1. GT-Power software 36
5.2. Sisudiesel 420 DWRIE modelling 37
5.2.1. Diesel injection 37
5.2.2. Turbocharger 37
5.2.3. Intercooler 39
5.2.4. Intake and exhaust manifold 41
5.2.5. Sisudiesel 420 DWRIE engine model 43
5.3. Modified engine modelling 45
5.3.1. Cylinders and engine 45
5.3.2. CNG 45
5.3.3. Fuel supply 46
5.3.4. Knocking phenomenon monitoring 47
5.3.5. Sisudiesel 420 DWRIE gas engine model 48
6. Engine simulation 50
6.1. Sisudiesel 420 DWRIE simulation 50
6.2. Modified engine simulation 52
6.2.1. Modified engine performance 52
6.2.2. Compression ratio values sweep 55
6.2.2.1. Parameter values justification 55
6.2.2.2. Output data 55
6.2.3. A/F ratio values sweep 58
6.2.3.1. Parameter values justification 58
6.2.3.2. Output data 59
7. Results and discussion 63
8. Conclusion 66
9. References 68

Appendix I. Calculations I
Appendix II. GT-Power simulation data IV
Appendix III. Sisudiesel 420 DWRIE performance XIV
Appendix IV. GT-Power shared folder XVI

LIST OF FIGURES

Figure 1 Drawing of Sisudiesel 420 DWRIE 5
Figure 2 Different views of lab Sisudiesel 420 DWRIE 6
Figure 3 Map of CNG stations in Finland.....12
Figure 4 Map of LNG stations in Finland - yellow highlighted 12
Figure 5 Spark Plug Fuel Injector design 20
Figure 6 Different views of Sandfirden Technics modified engine 22
Figure 7 Decision diagram for engine modifying strategies and concepts 23
Figure 8 Section of the Sisudiesel engine with the injector yellow highlighted 24
Figure 9 Sisudiesel 420 DWRIE injector holder body diameter 25
Figure 10 Impossibility to fit the spark plug and the gas injector in the existing diesel injector hole.....26
Figure 11 Gas engine diagram of the selected strategy.....29
Figure 12 Conventional coil-ignition system 31
Figure 13 Cylinder head gasket (yellow highlighted) disassembling 32
Figure 14 Schematic design of a Venturi mixer.....34
Figure 15 Venturi principle.....34
Figure 16 Integration of gas mixer in the engine 35
Figure 17 Turbocharger modelling.....38
Figure 18 Intercooler modeling.....40
Figure 19 General manifold.....41
Figure 20 Intake manifold modelling in GT-Power 42
Figure 21 Discretization of the intake manifold.....42
Figure 22 Exhaust manifold modelling in GT-Power.....43
Figure 23 Discretization of exhaust manifold 43
Figure 24 Sisudiesel 420 DWRIE engine modelling in GT-Power software.....44
Figure 25 Simulation in GT-Power of the fuel supply system 47
Figure 26 Gas engine modelling in GT-Power software.....49
Figure 27 Sisudiesel 420 DWRIE Brake Power curves from the simulated data – red – and the manufacturer data – blue 50
Figure 28 Sisudiesel 420 DWRIE Brake Torque curves from the simulated data – red – and the manufacturer data – blue 50
Figure 29 Power curves comparison from the original Sisudiesel 420 DWRIE and the gas engine 52
Figure 30 Torque curves comparison from the original Sisudiesel 420 DWRIE and the gas engine 53
Figure 31 Knocking Probability for different compression ratios of the gas engine 56
Figure 32 Effect of the compression ratio on the Brake Power curve of the gas engine 56

Figure 33 Effect of the compression ratio on the Brake Torque curves of the gas engine 57
Figure 34 Effect of the compression ratio on the fuel consumption of the gas engine 57
Figure 35 AFR of each case simulated of the gas engine 59
Figure 36 Effect of the AFR on the Brake Power curves of the gas engine.....59
Figure 37 Effect of the AFR on the torque curves of the modified gas engine.....60
Figure 38 Effect of the AFR on the Fuel Energy Entering Cylinder curves of the gas engine 61
Figure 39 Effect of the AFR on the Throttle Angle curves of the gas engine 61
Figure 40 Effect of the AFR on the Brake Specific Fuel Consumption curves of the gas engine ...61

LIST OF TABLES

Table 1 Engine type designation breakdown 5
Table 2 Sisudiesel 420 DWRIE engine specifications 6
Table 3 Diesel fuel requirements 7
Table 4 Natural gas typical composition 14
Table 5 Properties of CNG, diesel and gasoline 15
Table 6 Limit values for Wobbe Index and Methan Number 16
Table 7 Main gas engine characteristics compared to the original Sisudiesel engine 30
Table 8 Values of compression ratio according to the thickness of the installed gasket 32
Table 9 Main gas engine parameters related to compression ratio reduction (see Appendix I). 33
Table 10 Turbocharger modelling parts 38
Table 11 Intercooler modelling parts 40
Table 12 CNG reference object 46
Table 13 CNG composition inputted in the model 46
Table 14 Knocking monitoring object 48
Table 15 Range of compression values to be simulated 55
Table 16 Range of AFR values and their percentage difference to the stoichiometric value to be simulated 58

GLOSSARY

AFR	Air-fuel ratio
BSFC	Brake Specific Fuel Consumption
CI	Compression Ignition
CNG	Compressed Natural Gas
CR	Compression Ratio
DI	Direct Injection
ECU	Electronic Control Unit
GHG	Greenhouse gases
IC	Internal Combustion
IDI	Indirect Injection
LNG	Liquified Natural Gas
LPG	Liquified Petroleum Gas
MN	Methane Number
NG	Natural Gas
SI	Spark Ignition
SPFI	Spark Plug Fuel Injector
TDC	Top Dead Centre
WI	Wobbe Index

1. Introduction

Internal combustion (IC) engines powered by liquid fuels are currently the main propulsion system in road transport (Serrano, et al., 2019) being responsible for about 10% of the world's greenhouse gas emissions (GHG). Moreover, they emit NOx and particulate matter which causes bad air quality in cities. Thus, in the last years, it has been a goal for researchers to mitigate the environmental impact of road transport, by reducing fuel consumption and emissions of the IC engines (Reitz, et al., 2020). Besides, the reputation of IC engines, and particularly diesel engines, has been compromised by emission scandals (Baumgärtner & Letmathe, 2020). For these reasons, several EU countries presented legislation plans to prohibit IC engines in their markets, and advocate for a transition to full electric mobility by 2040 (Wappelhorst, 2020). Likewise, some car companies such as Ford, Volvo, or Jaguar have already announced their intentions to only sell electric vehicles by 2030 in Europe (Frangoul, 2021).

Future trends in the transport sector are evidently inclined to electric mobility, but some challenges need still to be faced, such as battery technology or the recharging infrastructure (Chala, et al., 2018; Ghosh, 2020). And at this moment, the IC engine seems the more convenient option not only for road transport but also for a range of applications such as industrial usages (Reitz, et al., 2020). So, it is difficult to have a rapid transition from the traditional diesel and gasoline IC engines to fully electric mobility.

This evidences the need for a transition technology before the total implementation of electric mobility. A technology that can satisfy the applications for which IC engines are currently used and at the same time contributes to reducing GHG, NOx and particulate matter emissions. In this line, the use of alternatives fuels for powering IC engines can play a major role. For instance, natural gas is the fossil fuel that produces the lowest GHG emissions and the minimum level of suspended particles (Chala, et al., 2018). So, the implementation of these fuels in the current IC engines will provide a technology that enables extending the existing engines' life and avoids them being dismissed because of their emissions. Consequently, it is highly convenient to study and develop feasible, simple, and economical procedures to convert the existing engines to operate with these alternative fuels.

This thesis focuses on the case of implementing alternatives gaseous fuels, also known as fuel gases. Novia University of Applied Sciences, based in Vaasa (Finland), currently has a diesel engine (Sisudiesel 420 DWRIE) in the laboratory. It is used for simulation and analysis purposes. Then, if it had an engine powered by gas it would be possible to conduct investigations with this fuel. So, given the research and investigation interest in alternative fuels, it is desired to convert this existing diesel engine to operate with alternative fuel gas.

Therefore, this thesis aims to explore the possibilities of converting the laboratory diesel engine to a gas engine. The thesis defines a feasible engine concept so that the laboratory engine can fully operate on the previously selected appropriate gaseous fuel. It also models and simulates in GT-Power software the proposed gas engine.

2. Aims and objectives

The aim of this thesis is to evaluate which is the optimum solution when implementing a dedicated fuel gas engine in Novia UAS' laboratory - it is relevant to note that it is requested a gaseous type of fuel. The lab currently has a Sisudiesel engine, and it will be debated which is the best option to modify it to operate on fuel gas.

To achieve the aim of this thesis, the following objectives are defined:

- Analyse the existing engine in the laboratory and define how could be restructured to work with fuel gas.
- Research the available fuel gases that can be used in an internal combustion engine to decide which one fits better.
- Explore and compare diverse engine concepts and modifying strategies to adapt the lab engine to a dedicated fuel gas engine.
- Simulate the selected concept with the software GT-power simulation tool and evaluate how different parameters influence the engine performance.

3. Review of literature

3.1. Sisudiesel 420 DWRIE engine

The available laboratory engine in Novia UAS' laboratory to be converted to work on gas is a Sisudiesel engine. Specifically, the engine is called Sisudiesel 420 DWRIE and it is located in the Energy Technology and Automotive Technology laboratory in the basements of the Technobothnia building in the Finnish city of Vaasa. In section 3.1.2 is undertaken an analysis of this engine to know its designations and specifications.

3.1.1. AGCO Power Inc.

Sisu Diesel Inc. was the name of the company currently called AGCO Power Inc. from 1994 to 2009 (Porssitieto, 2021). This company have had different names since its first establishment in Siuro, Nokia, Finland, in 1942. Back then, the company goal was to repair and manufacture some aircraft parts and engines – it was the second-largest Finnish aircraft engine factory.

After the end of World War II, the company shifted its aircraft objectives towards developing, designing, and producing diesel engines, which is still the company aim. Nowadays the current company name is AGCO Power Inc., and it mainly develops diesel engines, highlighting three, four, six and seven-cylinder diesel engines for tractors, diesel marine engines and diesel power generation solutions (Agco Power, 2020).

According to Statista (2020), a distinguished German company specialized in the market and consumer data, Argo Power Inc. employed more than 21,000 people and had a financial turnover of 7,54 million euros by the end of 2020 – the latest year with available data. The company exports worldwide having 3,250 dealers around the world. Their current portfolio includes the manufacturing of tractors, combine harvesters, smart farming, and grain storage, among others (Agco Power, 2020).

The diesel engine from Novia UAS' laboratory to be converted to fuel gas was manufactured by Sisu Diesel Oy company.

3.1.2. Sisudiesel 420 DWRIE specifications

According to the plate in the Sisudiesel engine from Novia UAS' laboratory, the name of the engine model to be evaluated and studied is Sisudiesel 420 DWRIE (Figure 1). This type of engine is used mainly to supply tractors. The engine designation indicates the main characteristics of the engine, and they are summarized in Table 1. The engine specifications are indicated in Table 2.

Table 1 Engine type designation breakdown (Sisu Diesel Inc., 2002)

4	4 cylinders
20D	Basic type (not ECU)
W	Turbocharged engine equipped with bypass turbo
R	Rotary fuel injection pump
I	Equipped with intercooler air to water
E	Emission tested engine (certified) for off-road

From Table 1, it has to be highlighted that the engine does not equip an ECU (Electronic Control Unit) and that it is designed and certified for off-road applications.

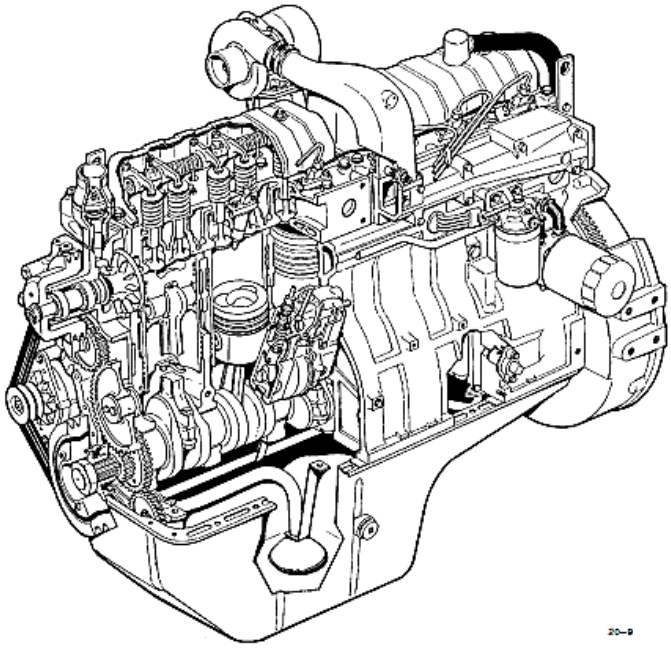

Figure 1 Drawing of Sisudiesel 420 DWRIE (Sisu Diesel Inc., 2002)

Table 2 Sisudiesel 420 DWRIE engine specifications (Sisu Diesel Inc., 2002)

Manufacturer	SISU Diesel Inc. (FINLAND)
Type	Sisudiesel 420 DWRIE
Power	95 kW at 2200 rpm
Serial nº	J18570
Displacement (dm^3)	4.4
Cylinder bore (mm)	108
Stroke (mm)	120
Compression ratio	16.5
Combustion	Direct injection
Firing order	1-2-4-3
Compression pressure (bar)[1]	24
Weight (kg)[2]	345
Direction of rotation from the engine front	clockwise

[1]) Minimum value at operating temperature and starting revs. Max permitted difference between cylinders 3,0 bar.
[2]) Without flywheel and electrical equipment.

This diesel engine was initially designed as a tractor engine and subsequently assembled in the laboratory for academic purposes. It has direct injection (DI) without a common rail. And according to the engine plate, it has an output of 95 kW (approx. 130 hp) at 2200 rpm.

Figure 2 shows the set-up of the lab Sisudiesel 420 DWRIE engine in the Energy Technology and Automotive Technology laboratory of Novia UAS.

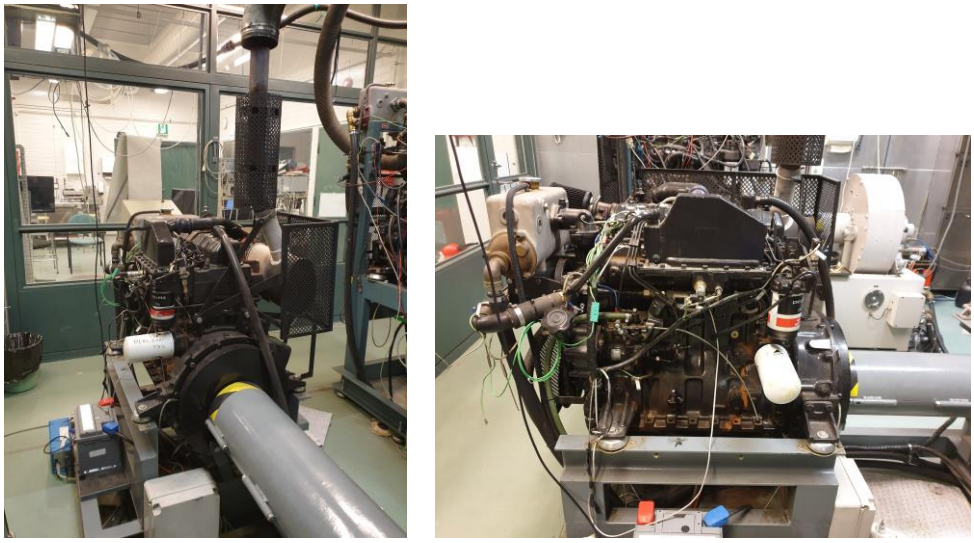

Figure 2 Different views of lab Sisudiesel 420 DWRIE

Notice the plentiful space both on the sides and above the engine that potentially could allow assembling all the possible necessary parts to convert the Sisudiesel engine to a dedicated fuel gas engine.

3.1.3. Diesel

Diesel – also known as gasoil or diesel oil – is the typical fuel used in diesel engines and, therefore, used in the Sisudiesel 420 DWRIE. It is obtained through crude oil distillation, it boils in the range of 175-345^{o}C and consists basely of hydrocarbons in the liquid state with ignition values of approximately 350 ^{o}C (Schobert, 2014).

According to Bosch (2014), high-quality types of diesel have the following peculiarities and attributes taking into account their service life and that the fuel-injection systems work in a constant function: high cetane number; moderately low final boiling point; low sulphur content; narrow density and viscosity spread; low aromatic compounds content; good lubricity; absence of free water; and restricted pollution with particulate.

Table 3 specifies the most relevant automotive diesel fuel requirements according to the European Committee for Standardization (2009).

Table 3 Diesel fuel requirements (European Committee for Standardization, 2009)

Standard	Unit	Parameter
Cetane number	-	≥ 51
Cetane index	-	≥ 46
Density at 15°C	kg/m^3	820-845
PAH[1])	% by mass	≤ 11
Sulphur content	mg/kg	≤ 10[2])
Flash point	°C	≥ 55
Total contamination	mg/kg	≤ 24
FAME content[3])	% by volume	≤ 7
Lubricity	µm	≤ 460
Viscosity at 40°C	mm^2/s	2-4,5

[1]) Polycyclic aromatic hydrocarbons which are defined as the total aromatic hydrocarbon content less the mono-aromatic hydrocarbon content.
[2]) EU proposal to have what is considered sulphur-free from 2009.
[3]) Fatty Acid Methyl Ester content.

3.2. Review of available fuel gases

According to the scope of this thesis – see aims and objectives in section 2 –, from Novia UAS' laboratory it is solicited to implement in the engine a gaseous type of fuel, which will be called fuel gas from now on.

As a fuel gas, it is understood a propellant that enters the engine in the gaseous phase although may be stored as a liquid to facilitate its storage. Therefore, CNG (Compressed Natural Gas) would enter the thesis' scope but for instance, biodiesel or alcohols do not. That is an important fact because a big delimitation of the fuels to be studied is made beforehand. Accordingly, it has been agreed that it will be studied the following fuel gas alternatives: biogas, natural gas (or biomethane) with its different storage forms, and liquified petroleum gas.

In order to achieve a good selection concerning the fuel gas that will be implemented in the laboratory engine, it will be broadly taken into account the supply and availability adequacy of the fuel gas; its ease of transport and safety of storage; the modifications needed in the engine; the engine efficiency; and the fuel gas compatibility with the engine (power, emissions, ease of use and durability of the engine). All these criteria based on Kumar (2018) and Ramadhas (2011) will be considered in the following subchapters.

3.2.1. Main characteristics of fuel gases

From the considered fuel gases, their main characteristics are discussed to see whether they are suitable for their implementation on the engine object of study.

3.2.1.1. Biogas

Biogas is a gas mainly composed of methane (40-75%) and carbon dioxide (15-60%). It can also contain traces of water vapour, N_2, O_2, H_2, H_2S (Ryckebosch, et al., 2011). It is obtained from the anaerobic digestion of biomass.

The gas quality requirements for an engine are strict. For example, high water or H_2S content imply corrosion (Wellinger & Lindberg, 2005) or high content of CO_2 can imply a lower calorific value (Ryckebosch, et al., 2011). So, it is not recommended to use raw biogas as an engine fuel. Instead, as suggested by Wayan Surata, et al. (2014) it must be improved before upgraded.

Nevertheless, the company Scania (2018) tested using raw biogas – without refining or upgrading – in their engines, but this is at a very experimental stage.

3.2.1.2. Natural gas and biomethane

Natural gas (NG) is a complex mixture of hydrocarbons in a gaseous state. It is primarily formed by methane (80-98%), but usually, it also includes ethane, propane, higher hydrocarbons, and other non-combustible gases (nitrogen, carbon dioxide) (Finnish Standards Association, 2017b). Regarding biomethane, according to Ryckebosch, et al. (2011) it is a gas composed principally of methane (95-97% CH_4 and 1-3% CO_2). It differs from natural gas because of its source. Biomethane can be obtained from the upgrade of biogas or methanation of bio-syngas (Finnish Standards Association, 2017a).

Natural gas and biomethane differ only on their source. As stated by IEA (2020), biomethane is indistinguishable from natural gas and compatible with natural gas vehicles (Chandra, et al., 2011). So, from now on, natural gas and biomethane will be named indistinctly.

Natural gas can be used as engine fuel for IC engines. However, according to the literature, lower engine performance is expected. Chandra, et al. (2011) observed, in comparison with diesel, a 31.8% power loss in the modified IC natural gas engine. Semin, et al. (2009b) concluded that a

modified gas engine implied a reduction in torque performance and Bari & Hossain (2018) also reported engine performance reduction. Moreover, a dedicated natural gas engine needs to have an ignition system such as spark ignition (SI) (Ramadhas, 2011; Chala, et al., 2018).

Due to natural gas low density, it is usually stored as CNG (Compressed Natural Gas) or LNG (Liquified Natural Gas) (Reif, 2015).

Compressed Natural Gas (CNG)

Natural gas can be stored in gaseous form at ambient temperature under high pressure (Ramadhas, 2011). It is compressed up to 200 - 248 bar (Imran Khan, et al., 2015) to obtain CNG – or compressed biomethane. Before handling it to the engine, it is converted to atmospheric pressure.

Liquified Natural Gas (LNG)

Natural gas and biomethane can also be stored in liquid form and atmospheric pressure. Liquified natural gas and liquified biomethane are obtained when they are cooled at cryogenic temperatures, about -161°C, and stored at atmospheric pressure (Ramadhas, 2011). LNG has a higher energy content per unit volume than CNG, but it presents more difficulties in storage. Although LNG tanks are well insulated, heat leaks into the tank and LNG start to evaporate. For this reason, LNG cannot be permanently stored (Go With Natural Gas, 2014). Furthermore, LNG has a higher cost of production and storage (Semin, et al., 2009a).

3.2.1.3. Liquefied Petroleum Gas

Liquefied petroleum gas (LPG) can be obtained from different sources such as natural gas purification, oil fields or as a by-product of petroleum refining. It consists of condensed butane (C_3H_8) and propane (C_4H_{10}) gases, with configurations for automotive fuel about 70% of butane and 30% of propane however, it depends on the composition stipulated in each country (Ramadhas, 2011).

Characteristics that make LPG a fuel suitable for internal combustion engines are its high-octane number – good for spark-ignited engines –, the possibility of transport and storage in the liquid state, lower cost per energy than gasoline, and fewer GHGs emissions.

Regarding LPG use in vehicles, according to Ramadhas (2011), it can be used both in spark ignition and compression ignition (CI) engines. In the case of SI engines, there is the possibility to convert them to dedicated LPG fuelled engine since LPG behaves very similarly to gasoline when injected into cylinders. On the other hand, in the case of CI engines, the solution is to perform in a dual fuel mode operation, where it is injected a mixture of LPG and air and a small amount of diesel called pilot that allows the auto-ignition (Ashok, et al., 2015).

3.2.2. Fuel availability

From the viable fuel gases to implement in the engine, it is discussed their availability.

Finland has a developed industry of biogas production (Gasum, 2021b; Bioenergia, 2021) with 63 biogas production plants and an annual production greater than 100 hm^3 in the year 2017 (Winquist, et al., 2019).

Natural Gas in Finland is imported – mainly from Russia – or produced by improving biogas (Gasgrid, 2021). There are numerous CNG stations as can be seen in Figure 3. For instance, Stormossen is a company based in the Vaasa region that produces CNG by improving biogas. BIG-BIOGAS is the company that sells Stormossen gas and has two CNG filling stations within 10 km of Vaasa city centre (STORMOSSEN, 2021).

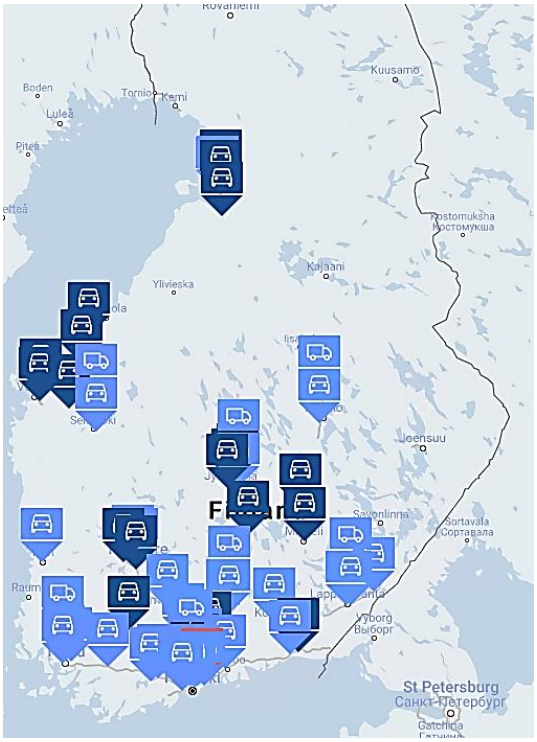

Figure 3 Map of CNG stations in Finland (Gasum, 2021b)

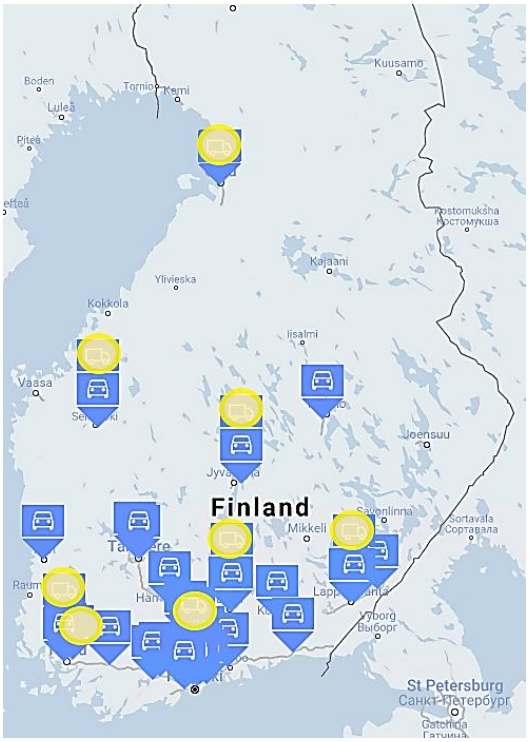

Figure 4 Map of LNG stations in Finland - yellow highlighted (Gasum, 2021a)

Some LNG stations can be found in Finland, as shown in Figure 4. But there are not so many stations as in the case of CNG. Moreover, the nearest station from Vaasa is about 80 km far.

Regarding LPG, it is not such an implemented fuel as natural gas in Finland (Salles, et al., 2019). Thus, there is not a developed LPG station network. However, it has been found that the company Teboil (2020) supplies LPG in little gas bottles, cylinders or tanks for companies or households.

3.2.3. Fuel gas selection

Biogas contains many impurities (Ryckebosch, et al., 2011) that can have bad consequences for gas infrastructure and the engine. Thus, it is not recommended to use untreated biogas in engines. For this reason, it is discarded as a possible fuel for being implemented in the engine object of study.

Although LPG is a fuel widely used for its properties and its possibilities of transport (Ramadhas, 2011), its uncommon supply in Finland – see section 3.2.2 – makes it not preferential for the chosen gaseous fuel.

In the case of LNG, it presents some difficulties in storing it permanently. The use of the engine, as a lab test engine, means that LNG would not be regularly consumed. So, for this reason, this fuel is dismissed as a suitable fuel for the lab engine.

So, for the arguments considered in sections 3.2.1 and 3.2.2, it is concluded that CNG is the more suitable fuel for implementing in the engine object of study of the present thesis, both for its characteristics and availability. It is suitable for the engine specifications and also widely available and locally produced in Finland.

3.2.4. Compressed Natural Gas

Compressed Natural Gas is natural gas that has been compressed to facilitate its storage. When stored it has a gaseous state, with pressures between 100 and 250 bar and temperatures between -40 to 30 °C (Chala, et al., 2018).

Natural gas

Natural gas is a gaseous mixture mainly composed of methane (CH_4), but it also contains certain amounts of ethane, propane, nitrogen, helium, carbon dioxide, hydrogen sulphide and water vapour. Natural gas varies in composition by location, season or even through the transmission network (Semin, et al., 2009c). However, a typical composition can be attributed to natural gas as seen in Table 4.

Table 4 Natural gas typical composition (Speight, 2015)

Constituent	Formula	Typical values (% v/v)
Methane	CH_4	70–90
Ethane	C_2H_6	0–5
Propane	C_3H_8	0–5
Butane	C_4H_{10}	0–5
Pentane	C_5H_{12}	0–5
Hexane (and higher)	$\geq C_6H_{14}$	Trace–5
Benzene (and higher)	$\geq C_6H_6$	Trace
Carbon dioxide	CO_2	0–8
Oxygen	O_2	0–0.2
Nitrogen	N_2	0–5
Hydrogen sulphide	H_2S	0–5
Rare gases	He, Ne, A, Kr, Xe	Trace
Water	H_2O	Trace–5

Table 4 shows that despite methane being the main component of natural gas, it can take a wide range of values of percentage by volume (from 70 to 90).

Natural gas properties

Natural gas properties play an important role in the different processes involved in the IC engine as mixture formation, ignition, and combustion. Table 5 shows a range of properties of CNG compared to traditional liquid fossil fuels Diesel and Gasoline.

Table 5 Properties of CNG, diesel and gasoline (Chala, et al., 2018)

Properties		**CNG**	**Diesel**	**Gasoline**
Chemical formula		CH_4 (83–99%) C_2H_5 (1–13%)	C_3 to C_{25}	C_4 to C_{12}
Composition by weight [%]	Carbon	75	87	85–88
	Hydrogen	25	30	12–15
Molecular weight [g/mol]		16.04	200	100–105
Density @15.5 °C [kg/m^3]		128	848	719–779
Stoichiometric air-fuel ratio	Molar Basis	9.7	50.03	59.5
	Mass Basis	17.2	14.7	14.7
Auto ignition temperature [K]		813.15	588.7	530.37
Octane number	Research octane number (R)	>127	N/A	90-100
	Motor octane number (M)	122	N/A	81-90
	Mean (R+M)/2	>120	N/A	86–94
Cetane number		N/A	40-55	5-20
Boiling temperature @atmospheric pressure [°C]		−164 to −88	180–340	27–225
Flammability of fuel - gas mixture [%]		5.3–15.0	1.0–6.0	1.4–7.6
Lower calorific value [MJ/kg]		47.13	42.78	43.44

The stoichiometric Air-Fuel Ratio (AFR) indicates the minimum amount of air needed for the complete combustion of the fuel (Çengel & Boles, 2014). Mass stoichiometric AFR for natural gas is 17.2, higher than in the case of diesel and gasoline.

Calorific value is the amount of energy released when a unit of mass of fuel reacts with oxygen in a combustion process (Mohamad, 2006). The calorific value of natural gas is higher than the value for gasoline and diesel.

Natural gas has a higher-octane number (127) when comparing it to gasoline (90-100). This means that natural gas is more resistant to the knocking phenomenon (Semin, et al., 2009c).

Flammability indicates the capacity of a fuel-air mixture to produce a flame that can propagate through the unburned mixture (Gardiner, et al., 2008). Flammability limits are the fuel concentration limits within the mixture is flammable. As seen in Table 5, these limits are higher for natural gas, which means it is less flammable than diesel or gasoline. In this line, Mohamad

(2006) suggests that, in IC engines, the ignition must be advanced earlier to ensure complete NG combustion.

Compared with Diesel, the higher autoignition temperature and the much lower cetane number indicate that natural gas requires higher ignition energy.

As stated, natural gas can vary in composition. Thus, two parameters allow defining and characterizing each specific natural gas. They indicate gas interchangeability and compatibility. These are the Wobbe Index (WI) and Methane Number (MN). The WI represents the heating value of the natural gas and it is determined by its composition. The MN is a measure used for the knock rating of gaseous fuels (Malenshek & Olsen, 2009). The European Standard EN 16723-2:2017 establish limit values for these two parameters as automotive gaseous fuel specifications. They are listed in Table 6.

Table 6 Limit values for Wobbe Index and Methan Number – adapted from Finnish Standards Association (2017a)

Parameter	**Required values**		**Recommended values**	
	Minimum	**Maximum**	**Minimum**	**Maximum**
Wobbe Index (MJ/Sm^3) inferior	-	-	41.9	49
Methane Number	65	-	70	-

3.3. Engine modifications to operate on natural gas

In this section, it will be studied which modifications require a diesel engine to work on natural gas, according to the gas properties analysed in section 3.2.4, and how can they be implemented.

3.3.1. Natural gas engine requirements

According to the literature, there has been identified a set of modifications that need to be made to a diesel engine to operate with natural gas. These are:

1) Installation of an ignition system
2) Reducing the compression ratio
3) Installation of fuel supply and mixing system

Firstly, regarding natural gas properties exposed in section 3.2.4, it is necessary to have an ignition system (Chala, et al., 2018). This is due to the natural gas high autoignition temperature, which implies that it gas cannot be ignited by compression, as it is done in a diesel engine (Reif, 2014).

Knocking is a phenomenon that must be avoided in engines. Having low compression ratios (CR) tends to avoid this phenomenon, but at the same time, low CR reduces engine performance and efficiency (Aina, et al., 2012; Gnanamoorthia & Devaradjaneb, 2015). Natural gas does not require so low a compression ratio as gasoline (Reif, 2015) because it is more resistant to knocking (see 3.2.4). Nevertheless, the pressures reached in the diesel engine will be too high for operating on natural gas. So, according to Siripornakarachai & Sucharitakul (2007), to ensure proper combustion and avoid knocking, the pressure in the cylinder chamber needs to be reduced. In this line, von Mitzlaff (1988) suggested the reduction of compression ratio to 12 or less while Ramadhas (2011) stated that the compression ratio needs to have a value between 10 and 13, and Kumar (2018) opted to maintain the compression ratio within 9 and 13. Moreover, another modification to avoid knocking could be reducing the turbocharger pressure.

It is also necessary to replace the diesel injection system, with a supply system suitable for CNG. This system must be able to obtain an accurate air/gas mixture and supply it to the combustion chamber (von Mitzlaff, 1988).

3.3.2. Possible diesel engine modifications to operate on natural gas

This section explores the possible modifications that can be applied to the engine object of study to meet the requirements of a gas engine, exposed in section 3.3.1.

3.3.2.1. Ignition system

As stated, a natural gas engine requires an ignition system (Reif, 2015). Many authors such as Kumar (2018) or von Mitzlaff (1988) suggest implementing spark plugs to ignite the mixture, a system very similar to those found in gasoline engines. As the engine has four cylinders, it will be necessary to implement an ignition distributor system connected to the camshaft or the gear drive. Besides, with spark ignition, the air-fuel mixture must be close to stoichiometric (Stone, 2012).

Some authors also propose using another fuel to ignite the air-gas mixture, a system which is known as pilot injection (Prasad, et al., 2019; Xiang, et al., 2020). This concept would require using an air gas lean mixture. Besides, it would imply having to fuel systems – natural gas and diesel –, increasing the engine complexity.

3.3.2.2. Compression ratio reduction

Different methods can be applied to reduce the compression ratio. They essentially focus on increasing the cylinder clearance volume.

Piston modification

One method is to machine off material from the piston. By milling the piston head, a bowl shape can be created. Apart from increasing the volume, this resulting geometry helps to obtain a proper natural gas and air mixture (Shinde, 2012). Even that, this process could alter the dynamic balance in the engine. Moreover, the machining must be accurate for the cylinder head not to become so thin (von Mitzlaff, 1988).

Connecting rod modification

Another possibility is to modify the length of the connecting rod. By reducing its length, the cylinder volume will increase, resulting in a lower compression ratio. Nevertheless, according to Kumar (2018), this method can be very costly. And an imprecise design can cause vibration and thermal stress to the piston.

Cylinder head gasket

The literature also suggests replacing the cylinder head gasket with a thicker one (Krishna, 2018; Kumar, 2018). This would enlarge the combustion chamber. An equivalent option suggested by Siripornakarachai & Sucharitakul (2007) is to add a plate known as a head spacer, similar to having two head gaskets. Both options do the same function but having a gasket plus a spacer may increase the risk of leakage. Anyway, these solutions rely on the availability of these parts or the feasibility of manufacturing them.

Cylinder head exchange

Von Mitzlaff (1988) also proposes to exchange the cylinder head for one that offers a higher combustion chamber volume, as an optimal method. However, it is subject to the availability of this part.

3.3.2.3. Fuel supply and mixing system

For the gas supplying system, two different concepts are considered according to the literature. One option is to install gas injectors in the cylinder head, supplied by a gas rail. The other option is to implement a carburettor or an equivalent mixing device.

Gas injectors

The gas injectors concept is proposed by Kumar (2018). In this case, the gas is directed to the common rail which supplies the injectors, and there is one injector for each cylinder (Reif, 2015). Then, the mixture is formed in the intake manifold – indirect injection (IDI) – or in the combustion chamber – direct injection (DI) – (Mohamad, 2010). This option requires fitting both the gas injector and the ignition device in each cylinder. This means that the installation of injectors may require a new cylinder head which could be bought, if available, or manufactured, with its complex design.

To solve the problem of fitting both the injector and the spark plug one alternative solution is the Spark Plug Fuel Injector (SPFI). This is a device that integrates both the injector and the spark plug, as seen in Figure 5. It was developed as part of a Ph.D. Thesis (Mohamad, 2010), but it is at an experimental stage, not being commercially developed.

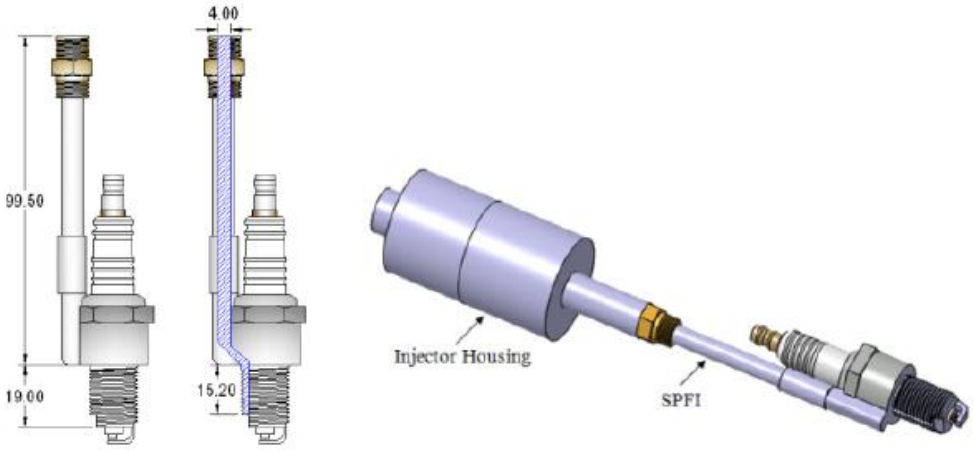

Figure 5 Spark Plug Fuel Injector design (Mohamad, 2010)

Mixing device

With the mixing device option, there is no need to install injectors. The air-gas mixture is formed in the mixing device before the intake port. So, no modifications would need to be done to the cylinder head. But it must be verified if it is physically possible in terms of available space to install this mixing device on the existing engine set-up. Besides, there are different options regarding the mixing device.

A simple mixing chamber such as a T-junction could be used to mix natural gas and air (Kok & van der Wal, 1996), in case the engine operates in steady conditions (von Mitzlaff, 1988). This means at constant speed and load. But the laboratory engine may be run at different speeds.

Another option is a Venturi mixer, as suggested by many authors such as von Mitzlaff (1988), Siripornakarachai & Sucharitakul (2007), Rodriguez Cussó (2013) or Sandfirden Technics (n.d.). The Venturi mixer uses the same principle as the carburettor.

3.4. SGI-4 industrial gas engine – a case study

Industrial gas engine SGI-4 is an engine concept developed by the Dutch company Sandfirden Technics. According to the personal correspondence with the company (12.4.2021), this new engine is manufactured based on the existing Sisudiesel DWRIE 420 engine.

The company designs and manufactures new cylinders heads with the necessary modifications to performance in natural gas. Moreover, some modifications are undertaken inside the pistons to get the desired compression ratios. Figure 6 shared by the company, illustrates the Sandifirden Technics engine which is quite similar to the lab Sisudiesel 420 DWRIE engine, however, an influential alteration has been carried out.

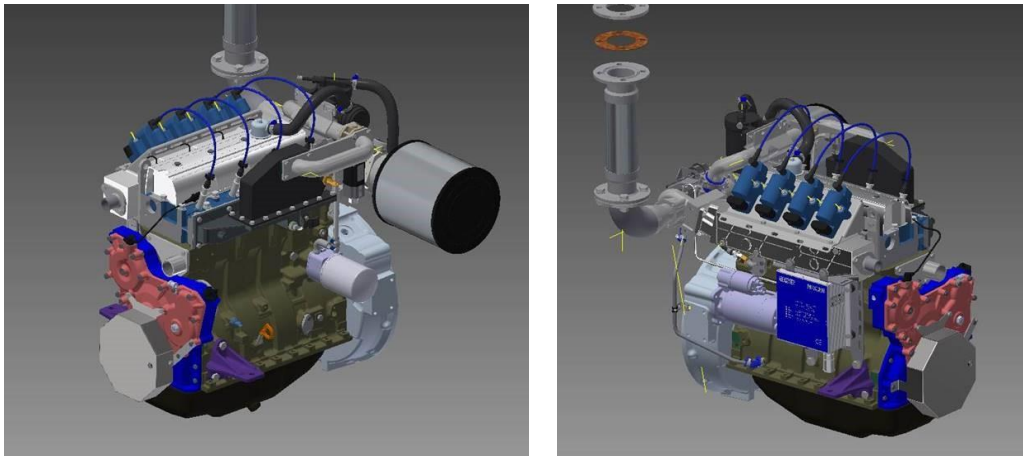

Figure 6 Different views of Sandfirden Technics modified engine (personal correspondence with the company, 12.4.2021)

The main modifications in the cylinder head are based on helping the engine to achieve a lower compression ratio and assembling a completely different injection system. As can be proved in Figure 6, no more direct injection is undertaken, and diesel injectors have been replaced by spark plugs since natural gas needs a spark to ignite. Instead, according to Sandfirden Technics (n.d.), a mixer type called Motortech VariFuel is used to blend the air and the natural gas in a manner analogous to the use of a carburettor in some liquid-fuelled engines.

Therefore, Sandfirden Technics has successfully achieved to modify existing Sisudiesel engines to work in fuel gas which can be considered a good inspiration for the present thesis.

4. Natural gas engine concept

4.1. Proposed strategies and concepts

In section 3.3.2, the required modifications for obtaining a gas engine are presented and different options to implement these modifications are discussed. These modifications need to be considered as a whole. Thus, three different possible engine concepts and modification strategies are proposed:

1) CNG SI engine with DI and the existing cylinder head
2) CNG SI engine with DI and a replaced cylinder head
3) CNG SI engine with air-mixing device

Figure 7 gives a picture of the available possibilities for converting the Sisudiesel engine to a dedicated fuel gas engine according to the reflections of section 3.3.2.

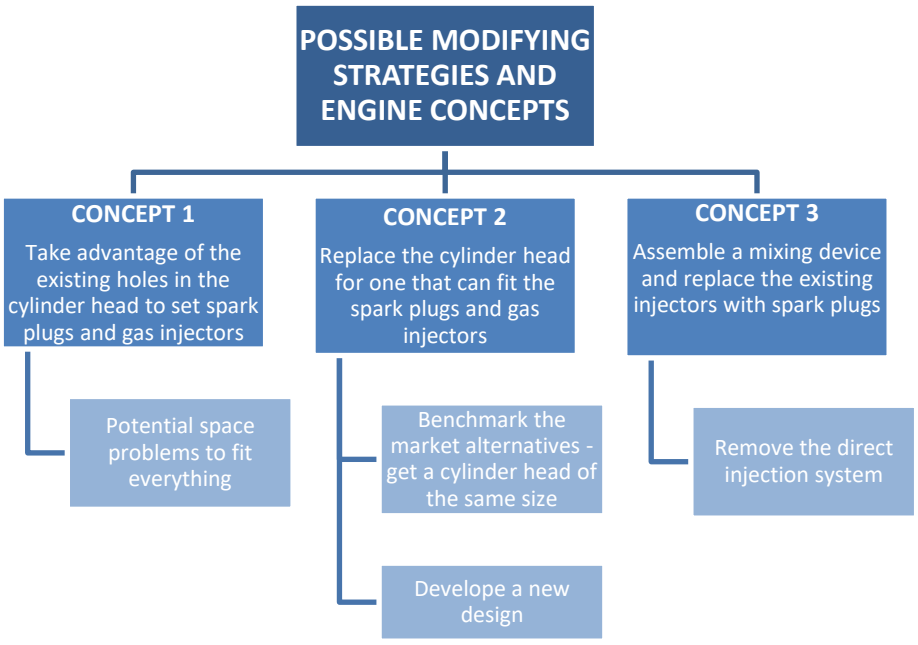

Figure 7 Decision diagram for engine modifying strategies and concepts

Throughout the current section, Figure 7 contents will be developed and discussed to achieve an optimal concept of dedicated fuel gas engines.

4.1.1. Concept 1. SI engine with DI and the existing cylinder head

Regarding the engine concept, the first strategy implies an SI engine equipped with a natural gas injection system with a common rail.

In the proposed strategy, the cylinder head is not replaced. Therefore, a head spacer should be installed to enlarge the combustion chamber and reduce the compression ratio. The thickness of this head spacer or gasket should be estimated and a market analysis carried out to obtain if it is manufactured. Otherwise, it would be possible to design and manufacture in detail a brand-new gasket in the university implying a high complexity level and demand which is out of the scope of this thesis.

The whole diesel injection system should be substituted for a gas injection system with common rail therefore the diesel injectors should be removed. As the cylinder head is not replaced, it should be managed to accommodate the new gas injectors and the spark plugs with the space left. And this is the point that would represent the greatest challenge.

Figure 8 shows the section of the Sisudiesel engine with the diesel injector.

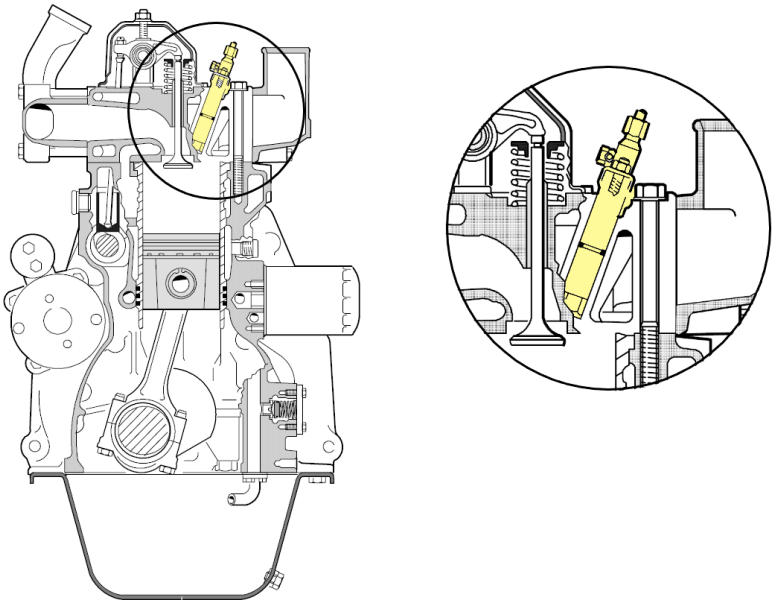

Figure 8 Section of the Sisudiesel engine with the injector yellow highlighted (Sisu Diesel Inc., 2002)

As seen in Figure 8, the injector highlighted in yellow is the one that requires replacement for both a spark plug and a gas injector. However, the existing injector holder body diameter is 21 mm (see Figure 9).

INJECTOR CROSS REFERENCE AND APPLICATION INFORMATION
(17, 17/21, and 21 mm Injectors)

Injector Part Number	Injector Inscription Code	Customer Part Number	Holder Part Number	Nozzle Part Number	Nozzle Inscription Code	Application
SISU DIESEL						
30105	—	BE 8368 40397	781649	30106	SDLLA 150S 30106	612 DS J L H.P.
33423	423	8368 54755	33424	33426	SDLLA 152M 33426	NA 20 Series
33780	—	8368 54786	781649	770620	SDLLA 150S 620	20 Series
33876	876	8368 54791	33424	33877	SDLLA 152M 33877	634 DSBIE & DWBIE
34358	358	8366 59808	33424	34359	SDLLA 152M 34359	420 DWRIE
34446	446	8368 54831	33424	34447	SDLLA 145M 34447	634 DSE
35234	234	8368 54929	33424	35235	SDLLA 145M 35235	645 Stage II
35300	300	8368 54936	33424	35304	SDLLA145M 35304	634-130 KW
35301	301	8368 54940	33424	35302	SDLLA 148M 35302	620-130 KW
35625	625	8368 54992	35624	35622	SDLLA 145M 35622	645 Stage II
35927	927	8367 64613	33424	35926	SDLLA 152M 35926	44 ETA

Figure 9 Sisudiesel 420 DWRIE injector holder body diameter – adapted from Stanadyne (2007)

Therefore, is evident that it is no viable to fit a spark plug and a gas injector in the existing diesel injector diameter. To demonstrate it, Figure 10 shows graphically the three diameters superimpose. The spark plug diameter corresponds to the model *CNG/LPG Laser Line* commercialized by the dealer NGK (2019) with a diameter of 14 mm. The gas injector is the *Fuel Injector High Impedance Gas Petrol Methanol* from the dealer Bosch (Bsuplemen, 2021) with a body diameter of 16 mm. Notice that thorough market research for the most feasible gas injector and spark plug has not been carried out since the objective is only to figure out the physical problem of space availability.

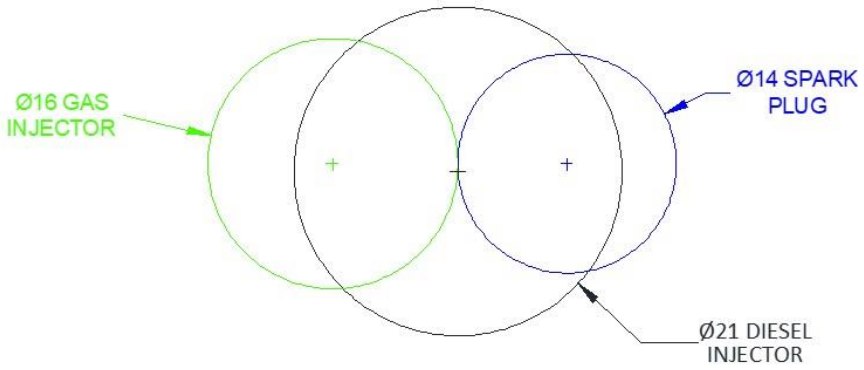

Figure 10 Impossibility to fit the spark plug and the gas injector in the existing diesel injector hole

Therefore, according to Figure 10, it is clear that there is no chance to fit the gas injector and the spark plug in the existing hole.

An alternative option could be the SPFI, which integrates both the spark plugs and injectors in a device (see section 3.3.2.3). But this part is at an experimental stage and it is not available in the market.

Finally, there are other points to focus on as well for instance the assembly of the gas common rail or the supply pump however, since it is a lab engine there would not be space problems to piecing together all that components.

Consequently, it is deemed this strategy to be not feasible to implement in the lab engine mainly for the impracticability to take advantage of the existing cylinder head for fitting both the spark plugs and gas injectors.

4.1.2. Concept 2. SI engine with DI and replaced cylinder head

In this case, the engine concept is the same as in the previous strategy. It is a SI engine with a natural gas injection system with a common rail.

The existing cylinder head is to be replaced. An appropriate new cylinder head could satisfy multiple requirements needed for the engine operation on gas. Firstly, it would allow having a larger combustion chamber, to obtain the desired compression ratio. Thus, there would be no need to add a head spacer. Secondly, the cylinder head could be designed to accommodate at the same time the spark plugs and the gas injectors. Moreover, the combustion chamber shape could be optimised to facilitate the air-gas mixture combustion.

This strategy requires having an appropriate cylinder head, which could be bought or designed and manufactured. Regarding the first option, it has been found that the company Sandfirden Technics (2020) has got modified cylinder heads for the Sisudiesel engine. These cylinder heads are specifically designed for engine operation on gas, but with a different engine concept (see section 3.4). Consequently, these cylinder heads are not adapted to lodge gas injectors. Furthermore, it has not been possible to verify its availability on the market.

This leads to the second option, to design and manufacture a new cylinder head. Designing such a complex part would imply a complex process, which is out of the scope of the present thesis.

So, for the unavailability of market supply of an adequate cylinder head, and the complexity of designing and manufacturing one, it is considered that this strategy is not effective for modifying the engine to operate on natural gas.

4.1.3. Concept 3. SI engine with mixing device

This strategy envisages an engine concept consisting of an SI engine with a Venturi mixer – gas mixer – as the natural gas supplying system. Thus, the obstacle of assembly of both the spark plug and gas injector in the existing diesel injector hole is dismissed.

In this case, the cylinder head is not replaced. Therefore, a head spacer should be installed to enlarge the combustion chamber and reduce the compression ratio. A gas mixer would be installed and since the air-gas mixture would be carried out there, all the current injection system should be disassembled. Thus, the existing diesel injectors would be removed, and the space left

would be utilised to install the sparks plugs since there would be no need to install injectors in the cylinder head.

This strategy requires replacing the cylinder head gasket with a thicker one or installing a cylinder head spacer. Any of these parts must be bought if available or manufactured. But in any case, designing and manufacturing them is much simpler than designing a whole cylinder head, as in the case of the second strategy proposed.

It has also been taken into consideration the characteristics of the engine – see section 3.1.2 –, such as that it does not equip an ECU.

In consequence, roughly, the use of a gas mixer, a gasket or cylinder head spacer, and spark plugs to convert the lab engine into a dedicated gas-fuelled engine seems to be an optimal and logical solution. Thus, this strategy is considered the most feasible according to the scope of this thesis and in section 4.2 it will be developed further.

4.2. Selected engine concept

According to section 4.1, the selected engine concept and modifying strategy is the third one. As stated previously, this strategy is to assemble a mixing device, replace the existing injectors with spark plugs and use a thicker head spacer to reduce the compression ratio. Specifically, the mixing device would be a Venturi mixer. Figure 11 shows the basics of the gas engine according to the selected strategy.

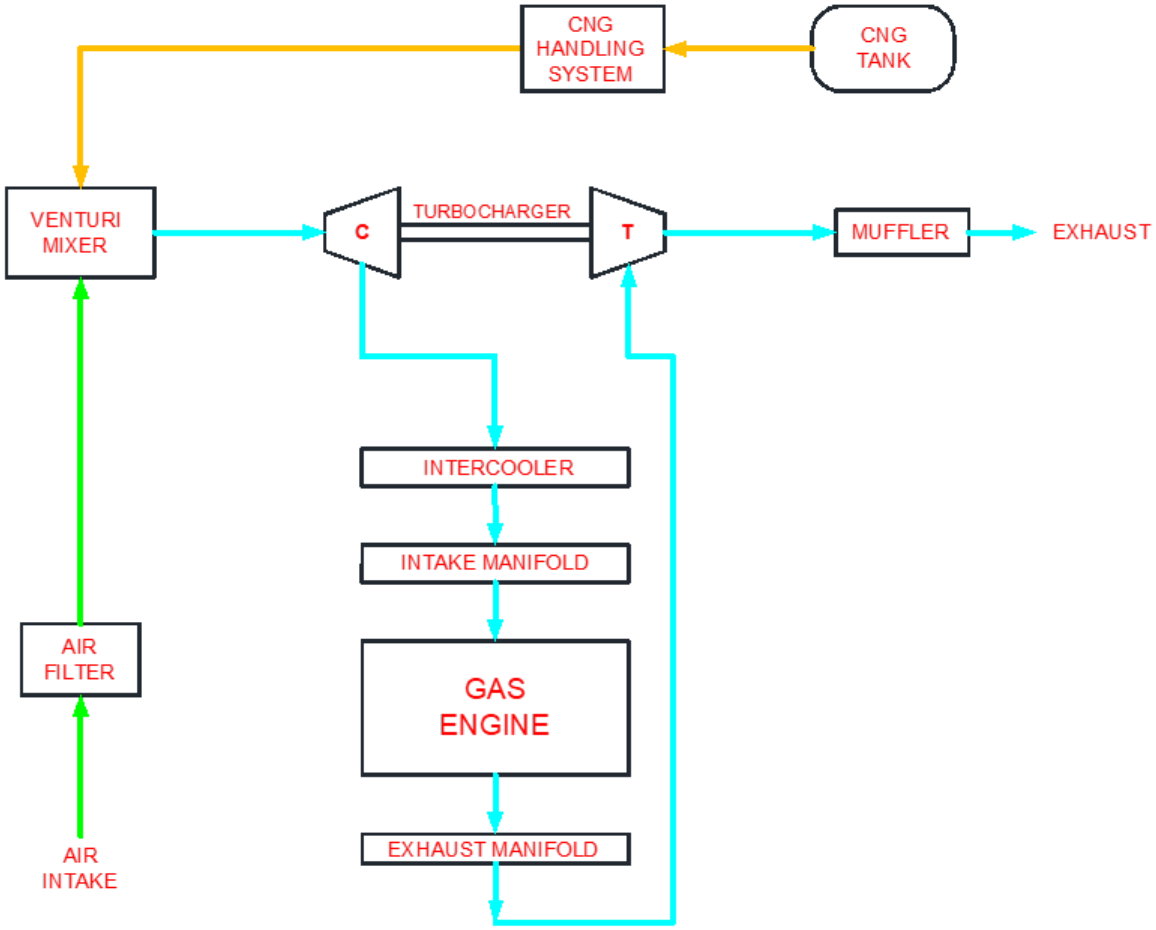

Figure 11 Gas engine diagram of the selected strategy

The resulting engine will have the specifications listed in Table 7. During this section, a detailed explanation of this strategy is to be undertaken.

Table 7 Main gas engine characteristics compared to the original Sisudiesel engine

Engine parameter	Sisudiesel 420 DWRIE	Gas engine
Bore (mm)	108	108
Stroke (mm)	120	120
Displacement volume (dm^3)	4.4	4.4
Compression ratio	16.5	10.13
Ignition type	Compression	Spark
Fuelling system	Direct Injection	Venturi mixer
Fuel	Diesel	CNG

4.2.1. Ignition system

The ignition system has the purpose of igniting the air-gas mixture in the combustion chamber. It must create a strong spark to ensure proper combustion of the mixture and fire this spark at the right time.

As the Sisudiesel 420 DWRIE engine does not equip an ECU, a fully mechanical system is chosen. So, the adopted solution is the installation of a battery ignition system, equipped with spark plugs and a distributor, known as conventional coil ignition (Reif, 2015). This system is mechanically connected to the engine.

It mainly consists of a battery that supplies a low voltage to the ignition coil. The coil steps up to higher voltage which is distributed to each spark plug by the distributor. Figure 12 shows a diagram of this ignition system.

1 Battery
2 Ignition/starter switch
3 Ignition coil
4 Distributor
5 Capacitor
6 Contact-breaker points
7 Vacuum advance mechanism
8 Rotor
9 Spark plug
1, 4, 15 Terminals

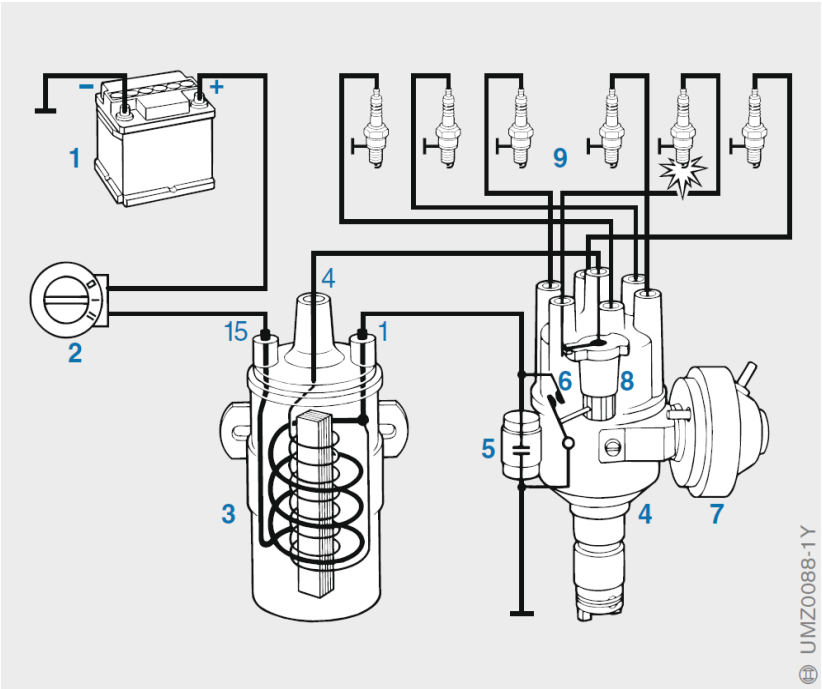

Figure 12 Conventional coil-ignition system (Reif, 2015)

The ignition system could be designed from zero, but also adapted from one used in another engine (Siripornakarachai & Sucharitakul, 2007).

4.2.2. Compression ratio reduction

To reduce the compression ratio, the cylinder head gasket will be replaced with a thicker one. This operation implies disassembling the cylinder head cover and the cylinder head. Then, the cylinder head gasket can be replaced.

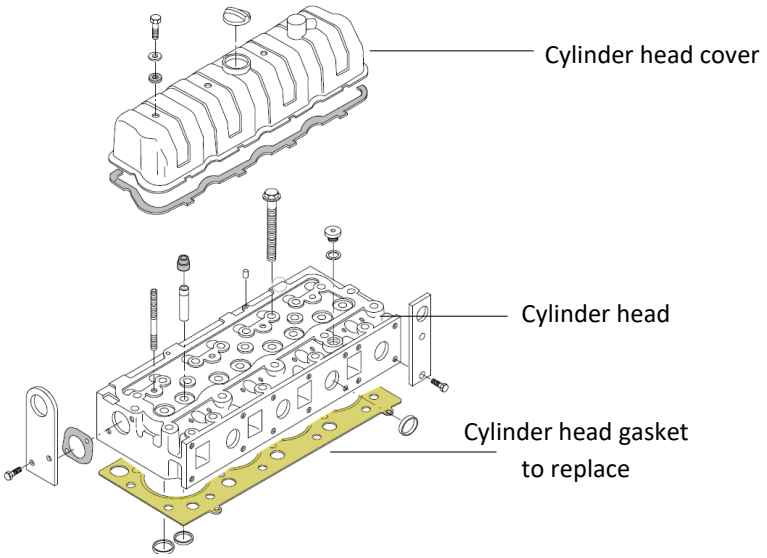

Figure 13 Cylinder head gasket (yellow highlighted) disassembling – adapted from Sisu Diesel Inc. (2002)

As stated in section 3.3.1 the value for the compression ratio should be between 10 and 13. But the exact value will depend on the new cylinder gasket thickness. It is considered that the cylinder gaskets can be obtained with a thickness precision of 0,5 mm. Therefore, Table 8 shows a range of gasket thickness values and the compression ratio that is obtained if installing them.

Table 8 Values of compression ratio according to the thickness of the installed gasket

New gasket thickness (mm)	r_C obtained
3	13.45
3.5	12.83
4	12.28
4.5	11.77
5	11.31
5.5	10.89
6	10.49
6.5	10.13
7	9.80
7.5	9.49
8	9.20
8.5	8.93
9	8.67
9.5	8.44
10	8.21
10.5	8.00

Compression ratio values from Table 8 are obtained according to the calculation methodology detailed in Appendix I, and assuming that the original Sisudiesel engine has a cylinder head gasket with a 1,1 mm thickness (Sparex, 2021).

Initially, a compression ratio value of 10.13 is chosen for the modified gas engine, as it is an enough low value that could guarantee margin against knocking, according to section 3.3.1. This compression ratio corresponds to a gasket thickness of 6.5 mm. So, the resulting values are listed in Table 9.

Table 9 Main gas engine parameters related to compression ratio reduction (see Appendix I).

Parameter	Value
Cylinder head gasket thickness	6.5 mm
Clearance height	13.155 mm
Compression ratio	10.13 mm

4.2.3. Fuel supply and mixing system

Regarding the fuel supply and mixing system, the solution selected is the installation of a Venturi mixer – also known as a gas mixer, or Venturi jet mixer, or gas carburettor – fundamentally because of the space availability, its simplicity and reliability since it is a device used for many years.

The existing supply and injection system must be disassembled. This means removing the injectors, the supply pumps, the various filters, and the pipes. Then the Venturi mixer will be installed. This device is to be installed between the air filter and the turbocharger to provide the air/gas mixture firstly to the intercooler and then to the intake manifold, as suggested in the research performed by Siripornakarachai & Sucharitakul (2007) and by the manufacturer Motortech (2018).

The gas mixer to be assembled is driven by almost the same physical principle as conventional carburettors. According to Grzywacz (2017), the gas mixer operates because of the fluid-mechanic

effect based on Bernoulli's principle of static pressure. As shown in Figure 14, the design of the converging part through which air (as the main fluid) passes makes an increase of the airflow velocity that causes a decrease in the air static pressure between the Venturi inlet (section 1) and the channel throat (section 2). That motives the suction effect of the passive fluid (CNG) which is aspirated in the mixing chamber in the required proportion and outputs on the diverging part with the proper air-fuel ratio.

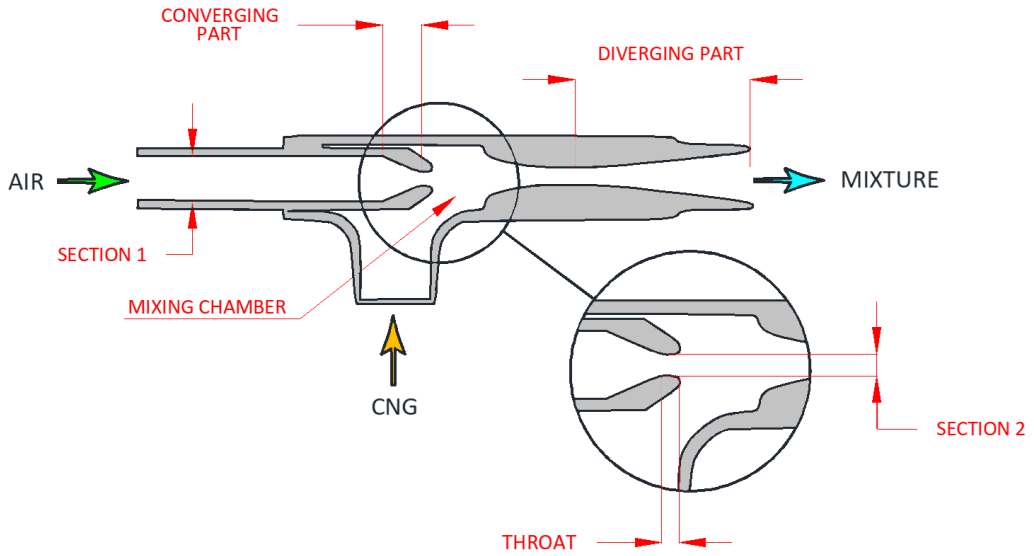

Figure 14 Schematic design of a Venturi mixer – adapted from Fox Venturi Products (2020)

The most typical gas Venturi mixers have multiple side orifices in the mixing chamber through the passive fluid can be suctioned. Figure 15 shows an outline of the Venturi principle.

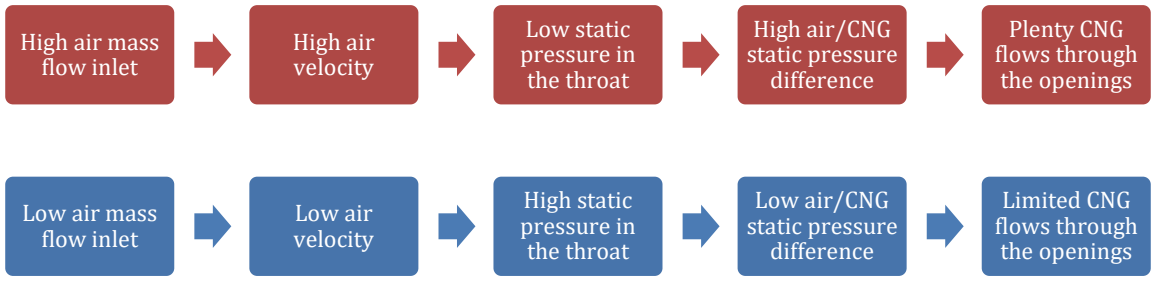

Figure 15 Venturi principle (Grzywacz, 2017)

Therefore, as explained in Figure 15, the Venturi mixer is considered a reasonable fuel supply solution since theoretically is capable to control by itself the gas amount to be injected. Siripornakarachai & Sucharitakul (2007) stated in their project to convert a diesel bus engine to work with natural gas that an optimal gas mixer for a natural gas engine should have a converging part of 40 mm of initial radius – section 1 of Figure 14 – and gradually narrowed with a cone angle of 10^{o}. Moreover, they stated as well that the air speed should be in a range of values between 100 and 150 m/s in the throat therefore, knowing the desired engine speed scope and the engine displacement volume, an approximation of the throat diameter – section 2 of Figure 14 – could be carried out to have an optimal gas mixer.

Finally, Figure 16 is roughly outlined how the installation of the gas mixer should be performed.

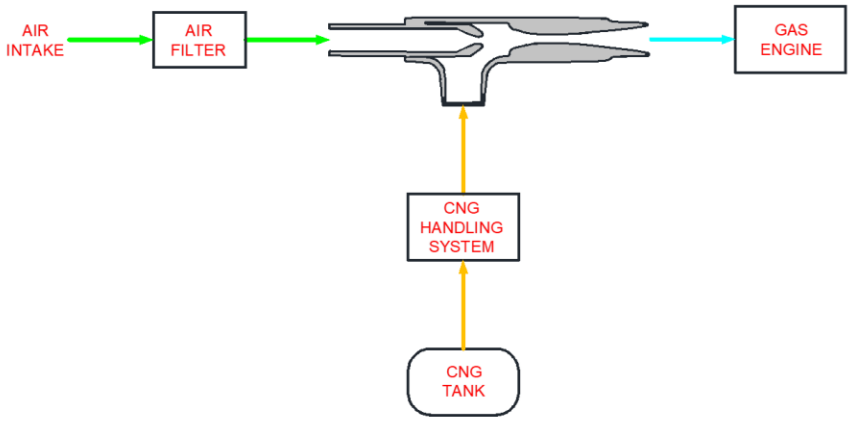

Figure 16 Integration of gas mixer in the engine

Initially, when simulating the modified gas engine an AFR ratio of 17.2 is to be established because according to Shimatsu (2017), close to it is where the CNG has the most stable combustion since this value is the stoichiometric air-fuel ratio. Thus, all the oxygen and all the fuel should be consumed during combustion.

5. Engine modelling

5.1. GT-Power software

GT-Power Engine Simulation Software has been selected to model the Sisudiesel 420 DWRIE engine and the different modifications to work on fuel gas because of its versatility, flexibility, and manageable graphic user interface. GT-Power is an internal combustion simulation tool developed by Gamma Technologies and matches perfectly with this thesis requirements since has a detailed cylinder model and a precise combustion analysis with both steady-state and transient simulation options.

According to Gamma Technologies (2021), GT-Power software is used by the vast majority of engine manufactures because it is able to model with a high level of detail all type of engines. It can predict accurately engines performance in terms of power, torque, fuel consumption, turbocharger performance, among others after asking for the introduction of plenty of precise data to adjust the results as much as possible to reality.

Finally, highlight the great capacity and adaptability of the software to display results in many different ways, always standing out clarity and visuality without losing efficiency and pragmatism. GT-Power, as part of GT-Suite, has a huge object library that offers a large number of modelling possibilities.

The software is based on modifying and completing existing templates from the *Template Library* to create objects that will be used in the model by dragging and dropping them in the interface's map zone. These objects – now parts – have to be linked with connection objects and the necessary properties for each component have to be defined. Before running the simulation, the user may determine the required output information and specify the run options.

5.2. Sisudiesel 420 DWRIE modelling

Modelling the Sisudiesel 420 DWRIE engine means not only to set into the software the engine specifications detailed in section 3.1.2 but also some other requirements which have to be measured from the environment – such as ambient temperature and pressure – or from the engine itself – such as some diameters and lengths. Furthermore, there has been personal correspondence with some companies from the engine manufacture sector to get some essential extra data.

In sections 5.2.1, 5.2.2, 5.2.3 and 5.2.4 are explained special components of this 4-stroke engine which are the injection, the turbocharger, the intercooler and intake and exhaust manifold. Moreover, in Appendix II it can be found a table with the basic simulation parameters while through Appendix IV is possible to acquire the GT-Power simulation files.

5.2.1. Diesel injection

Accurate knowledge of the amount of diesel delivered by the injectors into the cylinders is essential to obtain a reliable and realistic simulation. In the Sisudiesel 420 DWRIE engine, the quantity of diesel injected mass is 90 mg and in Appendix I all the calculations that support this value can be checked.

5.2.2. Turbocharger

Engine Sisudiesel 420 DWRIE is equipped with a turbocharger. As stated by Reif (2014), turbocharger forces under pressure the aspirated air into de cylinders in order to increase the air mass and, consequently, boost the fuel mass which entails a greater engine efficiency and engine performance both in terms of power and torque. A turbocharger takes advantage of the hot and pressured exhaust gases to drive a turbine at high speed and, through a shaft, the rotation generated is brought to the compressor which compresses the intake air.

As shown in Figure 17, the turbocharger is modelled in the GT-Power software basely linking the components compressor-shaft-turbine taking into consideration the compressor inlet environment conditions and turbine outlet environment conditions. Moreover, both inlet and outlet pipes of the compressor and turbine are set in order to let the flow pass through them.

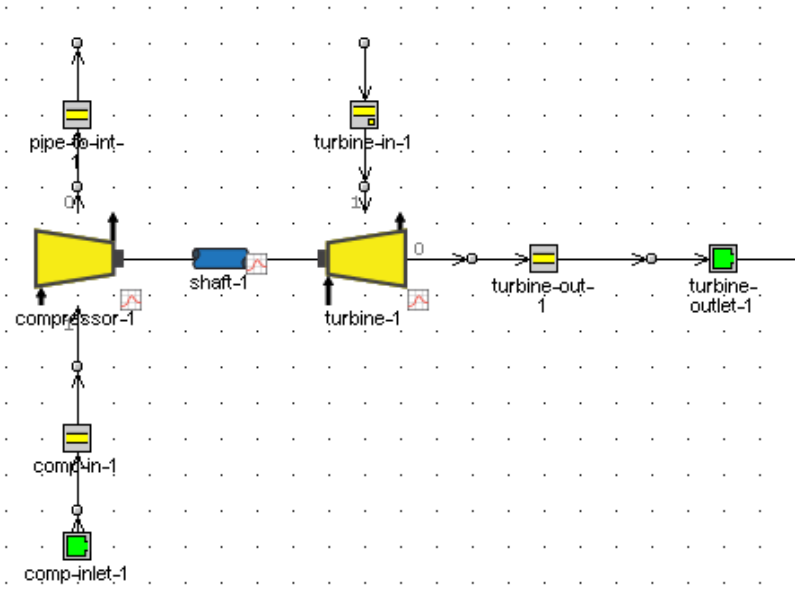

Figure 17 Turbocharger modelling

In Table 10, there is a simplistic explanation of all the items shown in Figure 17.

Table 10 Turbocharger modelling parts

Parts	Explanation
comp-inlet-1	Environment of the inlet air
comp-in-1	Pipe which brings the inlet air towards the compressor
compressor-1	Compressor
pipe-to-int-1	Pipe which drives the outlet compressor air to the intercooler
shaft-1	Turbocharger shaft
Turbine-in -1	Pipe that transports the exhaust gases towards the turbine
turbine-1	Turbine
turbine-out-1	Pipe which brings the outlet turbine air towards the outlet environment
turbine-outlet-1	Environment where outlet turbine gases are realised

Although the lab Sisudiesel engine is equipped with the turbocharger S1BG it has been possible to acquire neither the turbine and the compressor data map required by GT-Power nor shaft initial speed nor shaft moment of inertia. Some personal correspondence has been carried out with manufacturing companies of turbochargers such as Sandfirden Technics or Valmet but no success in terms of data obtaining was carried out. This is why the data maps of a turbocharger provided by GT-Power itself have been used – they can be checked in Appendix II. Emphasise that this turbocharger is manufactured for a 6-cylinders DI diesel engine which may disrupt the simulation results with the actual ones. Realize that this fact will have no effect on the conclusions reached in the thesis since both the modelling of the current engine and the modified engine will run with the same turbocharger.

5.2.3. Intercooler

Back to section 3.1.2, it has been detailed by the specifications of Sisudiesel 420 DWRIE engine manufacture that it has an intercooler air to water. Reif (2014) expounds on the need for the intercooler after the turbocharger compressor since in the compression process air is heated up – up to 180 ^{o}C. Sisudiesel engine intercooler cools down the compressed air with a separate water circuit before entering the cylinder in order to have denser air to increase the cylinder charge. Therefore, more oxygen is available for the combustion reason why greater power is obtained at a given engine speed.

GT-Power does not have an intercooler template by itself, that is why the intercooler is modelled treating it as a *black box*. As exposed in Figure 18, the modelling of the intercooler is based on the linking of several pipes which, adjusting their wall temperature and some reference objects, behave as a heat exchanger. The object IC-Eff comes from a template designed to impose cooler effectiveness with respect to the air mass flow at a given coolant temperature.

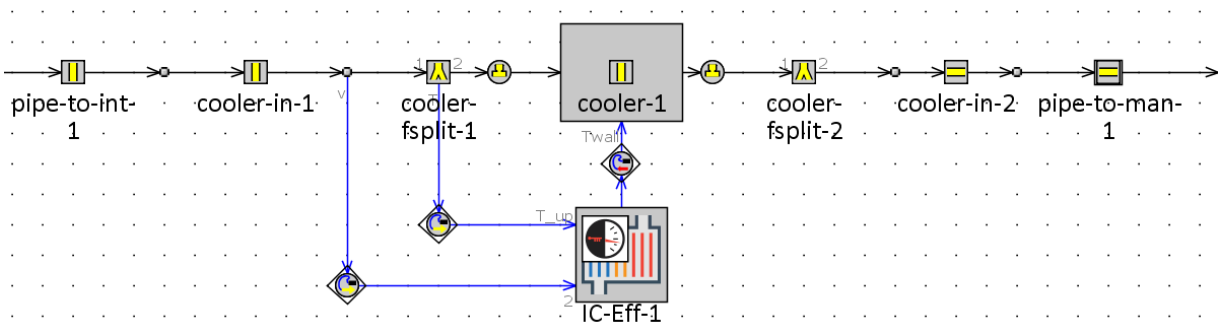

Figure 18 Intercooler modeling

In Table 11 it is a brief description of the main parts of the intercooler modelling according to Figure 18.

Table 11 Intercooler modelling parts

Parts	**Explanation**
pipe-to-int-1	Pipe which brings the air from the compressor towards the intercooler
cooler-in-1 cooler-fsplit-1 cooler-1 cooler-fsplit-2 cooler-in-2	Pipes and flow splits of the intercooler modelling
pipe-to-man-1	Pipe which leads the outlet air of the intercooler to the intake manifold
IC-Eff-1	Object to impose cooler effectiveness

5.2.4. Intake and exhaust manifold

Both intake and exhaust manifolds have to be discretised to achieve a good implementation in the GT-Power Software. The discretization process means dividing the physical volume of the manifolds into smaller sub-volumes by setting a series of general flow splits and pipes (Gamma Technologies, 2020). A general manifold can be conceived as shown in Figure 19.

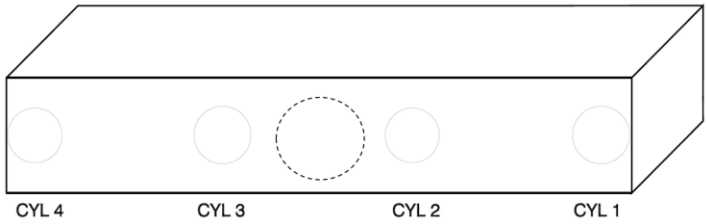

Figure 19 General manifold - adapted from Gamma Technologies (2020)

So, as exposed in Figure 19 four bores connect the manifold toward the cylinders and a big bore connects the manifold either to the intake system or exhaust system. That big bore is always located on the opposite surface from where the cylinder bores are placed since the flow enters through one side of the manifold and leaves through the other side.

For both the intake manifold and exhaust manifold it has been measured the total length, the diameter of the bore to cylinders, the diameter of the intake or exhaust bore and an approximation of the manifold diameter that is taken as a square to do the discretization – see the lateral parts of Figure 19**.**

In Figure 20 and Figure 21 it can be seen both the modelling of the intake manifold and its discretization. Notice the colour code that correlates the different parts between the figures. A brief explanation of how the discretisation has been done follows.

The yellow parts correspond to the main flow splits (*intman-fs*) that collect air from the intake manifold and distribute it to the cylinders. They have a volume of 480,000 mm^3 according to their dimensions 100x100x48 mm. The blue pipes (*intman-pipe*) connect the main flow splits, and the length of 86 mm is obtained through geometrical relation between the measurements.

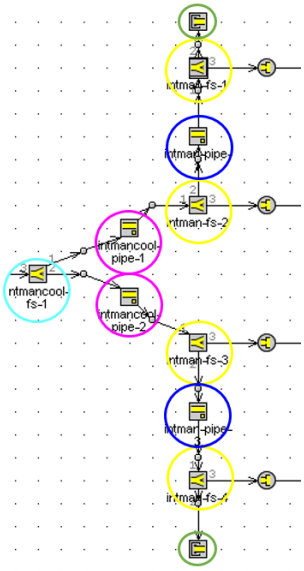

Figure 20 Intake manifold modelling in GT-Power

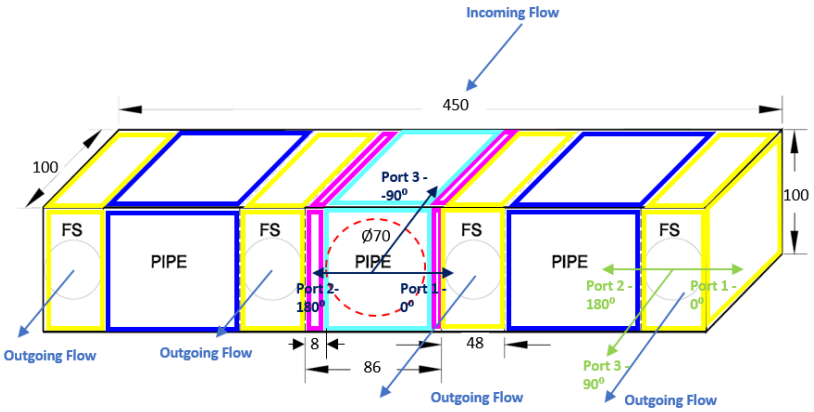

Figure 21 Discretization of the intake manifold - adapted from Gamma Technologies (2020)

Finally, the central part of Figure 21 is the volume where the inlet air from the intercooler enters – cyan section – and is flowed towards both sides – purple sections. The cyan volume (*intmancool-fs*) is a flow split of 700,000 mm^3 volume based on its dimensions 100x100x70 mm. The length of 8 mm of each of the two purple pipes (*intmancool-pipe*) is determined by geometrical relations between the lab measurements. The green circles of Figure 20 are *EndFlowCap* which are two objects that cap the third unnecessary port of the flow splits of the sides.

In reference to Figure 22 and Figure 23, in this case, they represent the modelling of the exhaust manifold and its discretisation, again notice of the colour code that links the parts of both figures.

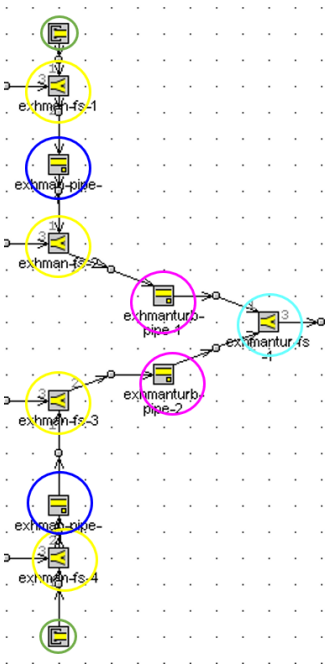

Figure 22 Exhaust manifold modelling in GT-Power

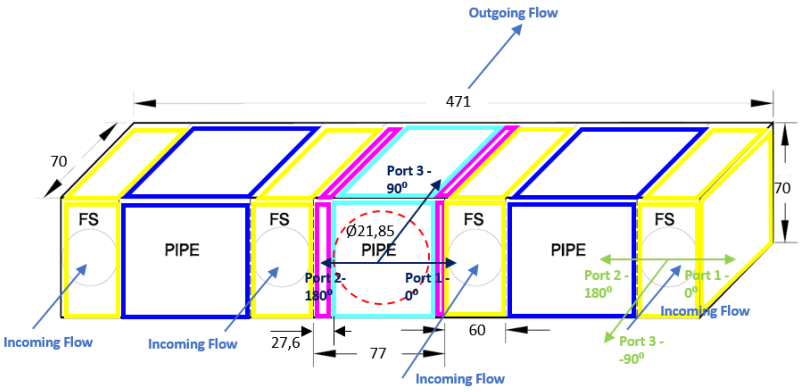

Figure 23 Discretization of exhaust manifold - adapted from Gamma Technologies (2020)

The discretization is completely analogous to the one undertaken in the intake manifold. The main difference between the intake manifold and exhaust manifold discretization is the direction in which the air flows. Figure 21 and Figure 23 have additional information concerning the orientation of the three ports of the flow splits which is essential for the modelling in GT-Power software.

5.2.5. Sisudiesel 420 DWRIE engine model

In Figure 24 it can be appreciated the definitive engine model of the original 4-cylinders Sisudiesel 420 DWRIE engine.

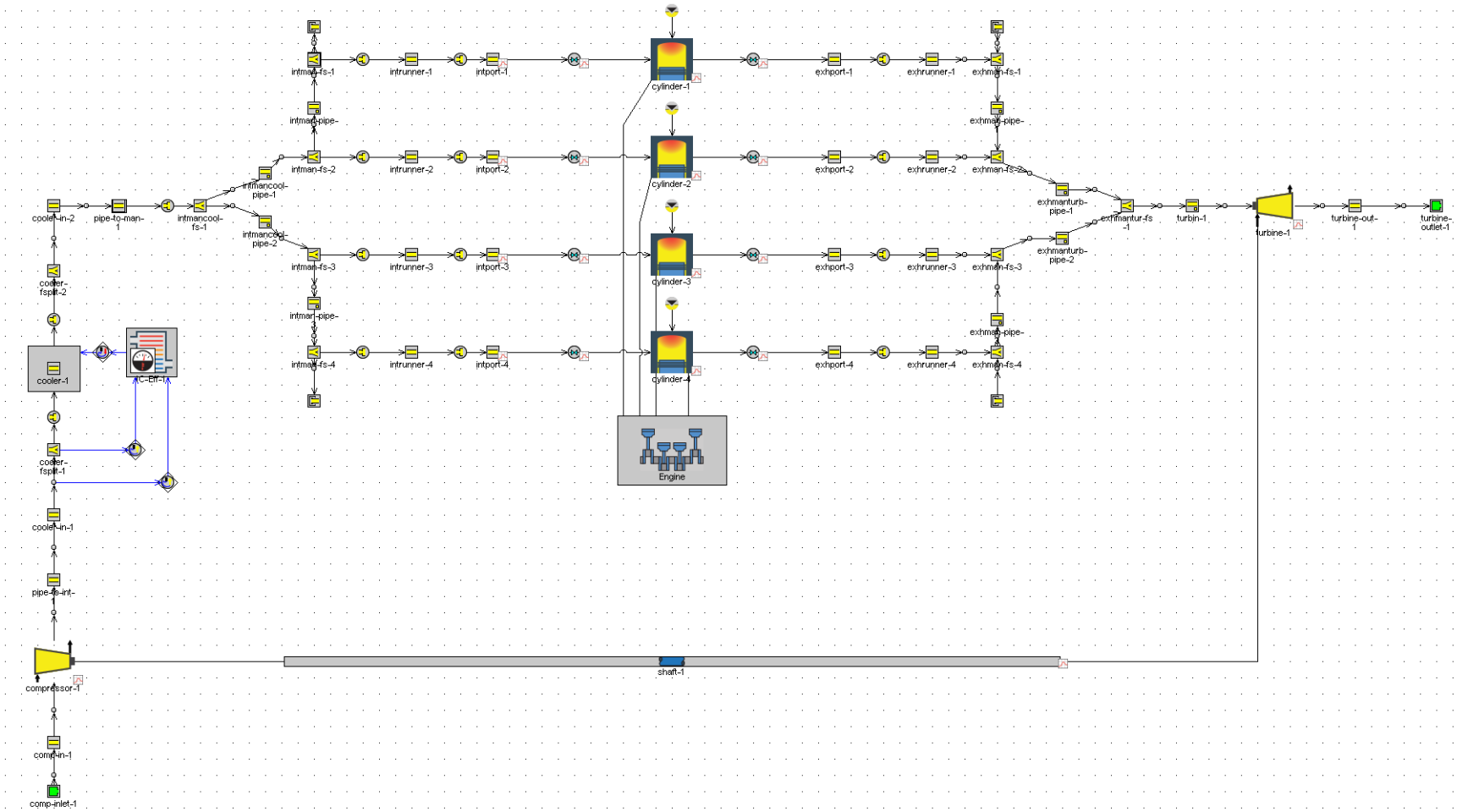

Figure 24 Sisudiesel 420 DWRIE engine modelling in GT-Power software

5.3. Modified engine modelling

The modified gas engine is to be simulated from the GT-Power model of the Sisudiesel 420 DWRIE engine carried out in section 5.2. The simulation of the Sisudiesel done will undertake some changes to run with CNG, the most significant ones will be described in the current chapter. Moreover, in Appendix II it can be found a table with the basic simulation parameters while through Appendix IV is possible to acquire the GT-Power simulation files. Notice that most of the modifications do not have a visual effect on the model since after all, the engine parts are almost the same.

5.3.1. Cylinders and engine

As stated in section 4.2, CNG demands spark plugs to ignite and perform proper combustion, so the combustion is changed from a CI to a SI designing a new combustion object in the cylinders called *gas_Comb*. Moreover, the compression ratio is required to be reduced, thus according to section 4.2.2, it is set to a value of 10.13 although is subject to further changes when simulating. To achieve it, modifications are undertaken in the Cylinder Geometry Object setting the desired compression ratio and a TDC Clearance Height of 13.155 mm according to the calculations carried out in Appendix I.

5.3.2. CNG

A CNG reference is created with the data of Table 12 and with the composition detailed in Table 13, according to the specifications of section 3.2.4.

Table 12 CNG reference object

Template	FluidMixtureCombined
Object Name	Natural_gas

Table 13 CNG composition inputted in the model

Fluid object	Mass or volume fraction	Molar fraction
Methane	0.88	0.943
Ethane	0.06	0.034
Propane	0.06	0.023

The CNG object (Table 12) is set in the inlet environment of the fuel supply, modelling the gas that would come from a tank. Moreover, all parts downstream of the Venturi mixer until the cylinders have an initial condition inside them of a mix of air (96.3%) and CNG (3.7%). That initial condition *FluidInitialState* is set as a reference object that describes the initial conditions inside that parts to start the simulation.

Based on its composition (Table 13) the CNG Methane Number (MN) is 81.9. This value is calculated using the online tool from Cummins Westport (2018), which outputs the MN from the molar fraction values. The MN value is within the limits, according to standards (see section 3.2.4).

5.3.3. Fuel supply

The Venturi mixer is modelled through a template called *FlowSplitTRight* which is basically a T-junction called *Venturi*. As can be checked in Figure 25, the atmosphere air inlet is through port 1, the CNG inlet is via port 3 and the outlet mixture is across port 2. To simulate in the gas mixer the appropriate Venturi effect, a Controller (*AFRController*) and a Throttle (*AFRthrottle*) are assembled between the CNG source (*Natural-gas-env-1*) and the Venturi mixer. The stoichiometric AFR target of 17.2 (see section 4.2.3) is set in the object *StoichFuelFlowTarget* although is subject to further changes when simulating.

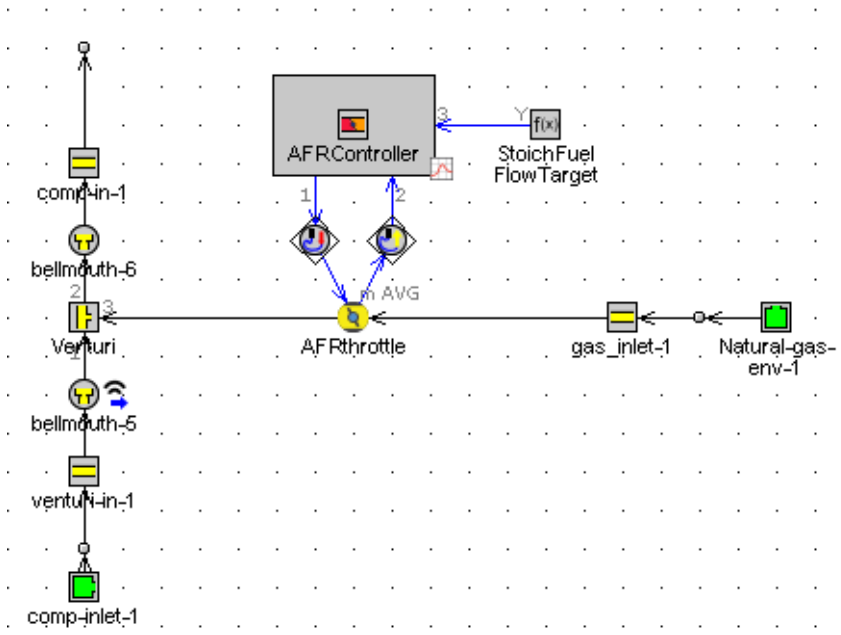

Figure 25 Simulation in GT-Power of the fuel supply system

According to Figure 25, the device works in such a way that the *StoichFuelFlowTarget* obtains the engine air inlet flow information from the *bellmouth-5* orifice and acts on the controller to change the throttle angle in order to provide the necessary gas flow to the Venturi mixer to maintain the desired AFR.

5.3.4. Knocking phenomenon monitoring

To control the knocking phenomenon in the engine, a reference object is created which will be called during the combustion simulation. This object uses the Knock Model *Kinetics-Fits-Natural-Gas*, which is suitable for natural gas engines. Table 14 details the specifications of this reference object.

Table 14 Knocking monitoring object

Template	EngCylKnock
Object name	Knocking
Knock model	Kinetics-Fits-Natural-Gas
Fuel methane number	81.9

This reference object is configured to only monitor knocking and output it. But it does not affect the simulation or varies other parameters in case of noticing the knocking phenomenon.

5.3.5. Sisudiesel 420 DWRIE gas engine model

In Figure 26 the definitive 4-cylinders Sisudiesel 420 DWRIE gas engine model can be seen.

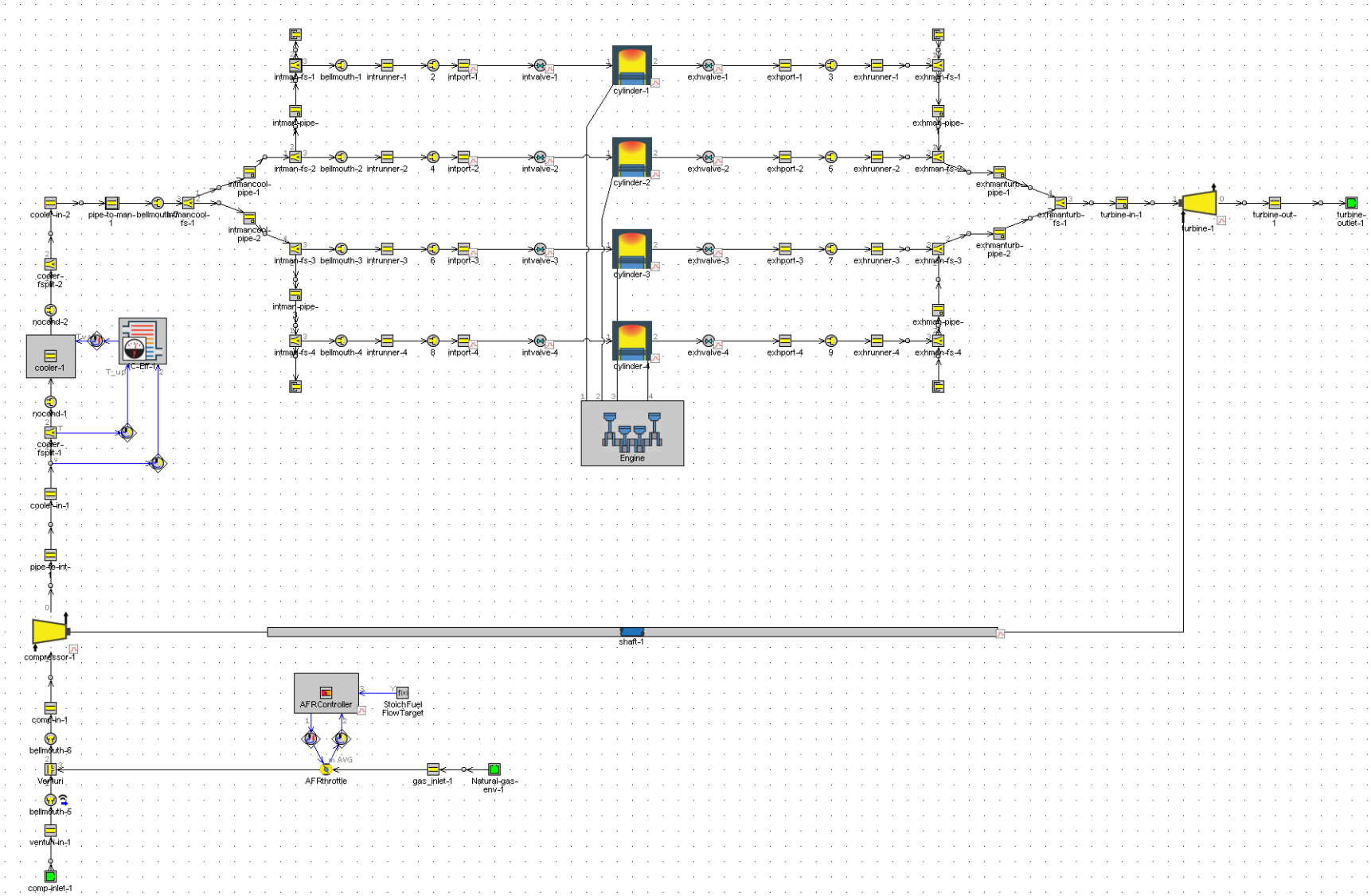

Figure 26 Gas engine modelling in GT-Power software

6. Engine simulation

6.1. Sisudiesel 420 DWRIE simulation

The Sisudiesel modelled engine has been simulated running at different speeds from 1000 to 2600 rpm (with a 200-rpm increment). Figure 27 and Figure 28 respectively show the power and torque curves obtained in the simulation – red lines – compared to those provided by the manufacturer (see Appendix III) – blue lines.

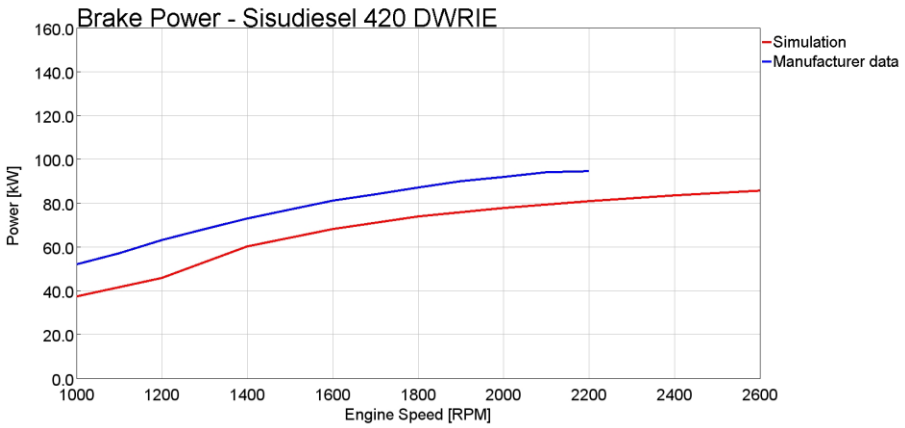

Figure 27 Sisudiesel 420 DWRIE Brake Power curves from the simulated data – red – and the manufacturer data – blue

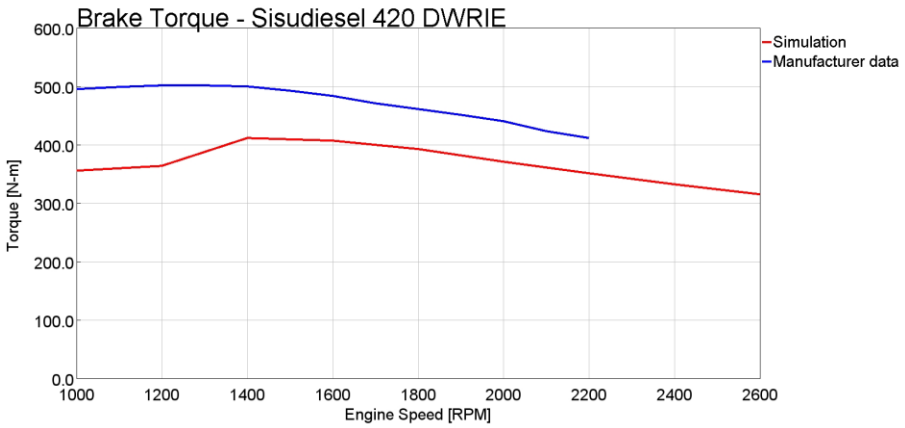

Figure 28 Sisudiesel 420 DWRIE Brake Torque curves from the simulated data – red – and the manufacturer data – blue

According to Figure 27 and Figure 28, it can be stated that both simulated curves have high similarity with the ones from the manufacture, with almost the same shape. However, a little anomaly in the simulation curves between 1000-1400 rpm can be appreciated in both figures fact that is blamed for a simulation error since the irregularity is slight.

Notice that both power and torque simulation data are about 15% lower than those provided by the manufacture – comparison data is taken at 1800 rpm. That little difference is attributed mainly to the fact that the turbocharger simulated is not the same as in reality. As mentioned in section 5.2.2 it has not been possible to get data from the real turbocharger. Therefore, it has been implemented a 6-cylinder turbocharger acquired from the GT-Power itself. Nevertheless, the thesis aim is not affected by this fact since the discussion of the gas engine setup will be always with the same turbocharger. Moreover, the impossibility to physically measure some parts of the engine is another element that may have its degree of responsibility in the results. The solution carried out has been to get that data from that parts from GT-Power tutorials and likewise that in the turbocharger case, it will not have any effect in the thesis aim since gas engine setup will always have the same physical data.

Therefore, it can be stated that the result of the Sisudiesel 420 DWRIE simulation is very close to reality. It can be considered a great and valid reference to set as a starting point to modify, in order to simulate a gas engine.

6.2. Modified engine simulation

The engine initial configuration is the one stated in section 4.2. This configuration is to be simulated to compare with the Sisudiesel engine simulation results (see section 6.1).

Further on, the current section is to undertake variations to decide the most optimal gas engine setup. The simulation is to be focused on two variables: the compression ratio (CR) and the air-fuel ratio (AFR). It will be used the ceteris paribus method to get results. Therefore, in the first simulation profiles, all variables are to be insulated except the compression ratio that is to vary within the literature proposed range (see subsection 6.2.2). In the second simulation profile, the variable to modify is the air-fuel ratio also within the literature suggested span (see subsection 6.2.3).

6.2.1. Modified engine performance

The gas engine is simulated to check its performance and compare it with that of the original Sisudiesel engine. To conduct this study, power – Figure 29 – and torque – Figure 30 – curves from both engines are to be plotted.

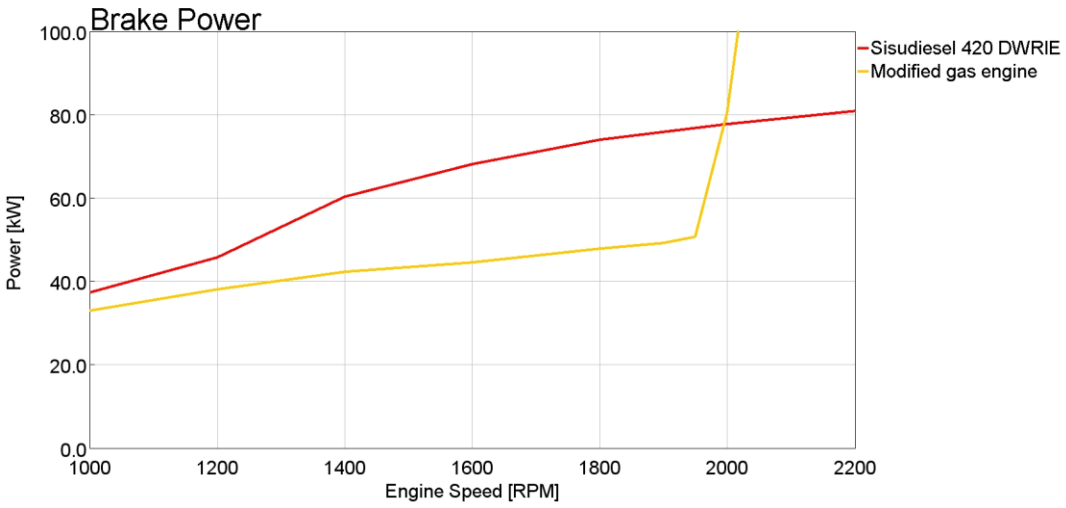

Figure 29 Power curves comparison from the original Sisudiesel 420 DWRIE and the gas engine

Figure 29 shows that both power curves have a similar shape and tendency. The power increases with speed in both cases. However, the modified engine has less power compared to the Sisudiesel. This is valid for nearly the whole range of engine speeds that the simulation has been conducted. But, while at low speeds (around 1000 rpm) the engines power outputs are very similar, the differences become more evident at higher speed.

It is noticed that, in the case of the modified engine power output (yellow curve in Figure 29), the results show an anomaly starting from the engine speed of 2000 rpm. This curve reaches a sudden value higher than 80 kW, coming from an output lower than 60 kW at about 1900 rpm, which is an unrealistic increase.

If dismissing this value, it is obtained that the modified engine has a power output ranging approximately from 33 to 50 kW, while the diesel engine goes from 37 to 78 kW. This means that the modified gas engine has between 10-35% less power than the Sisudiesel engine –depending on the engine speed point at which the data is compared.

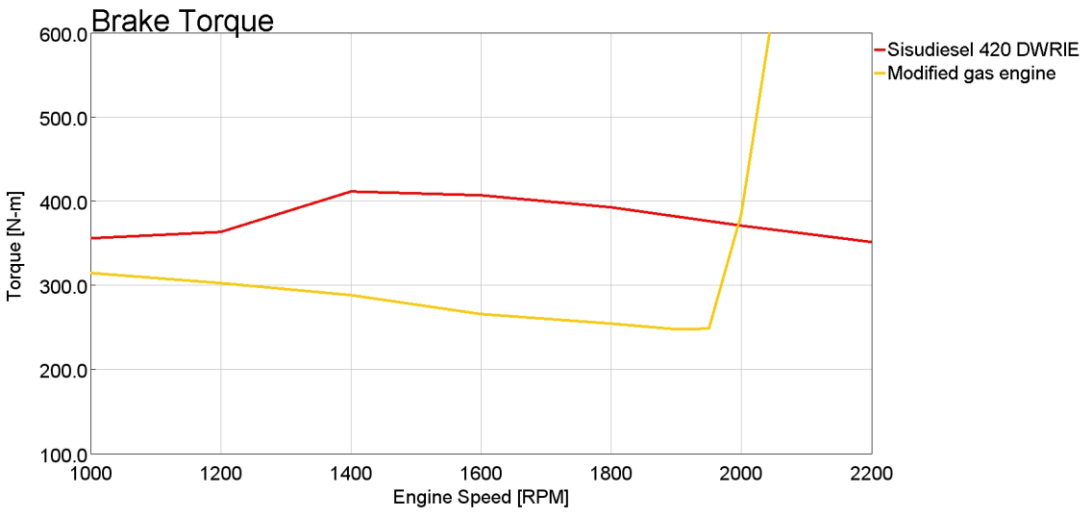

Figure 30 Torque curves comparison from the original Sisudiesel 420 DWRIE and the gas engine

In Figure 30 it can be seen that similar to what happens with power, the modified gas engine has less torque. In this case, some differences can be appreciated in the curve shapes and tendencies.

Whereas the diesel engine has the higher torque at about 1400 rpm and then it starts to decrease, the modified engine has its maximum torque at 1000 rpm and constantly decreases for the whole simulation until it reaches a speed of 1900 rpm.

It is from this point of 1900 rpm that the same anomaly as in the case of the power graph (Figure 29) can be found. Torque also shows a sudden increase, which may not be realistic. If data from this value are dismissed, the modified engine has a torque output ranging approximately from 314 and 248 Nm, while the diesel engine goes from 411 to 356. Therefore, the modified gas engine has between 12-33% lower torque performance than the Sisudiesel engine – depending on the engine speed point at which the data is compared.

According to the data exposed in Figure 29 and Figure 30, simulation results for engine speeds higher than about 1900 or 2000 rpm, are unrealistic. For this reason, in the following simulations, the range of speeds will be limited between 1000 and 1900 rpm, and the results out of this range are dismissed.

Therefore, in accordance with all that has been discussed in this section, the data from the modified gas engine is considered coherent and valid. According to the literature, a lower modified gas engine performance with respect to the diesel engine was expected. Thus, gas engine data obtained in the current section is to be used as a basis for the simulations in sections 6.2.2 and 6.2.3.

6.2.2. Compression ratio values sweep

Different values of compression ratio are considered, to analyse their influence on the gas engine performance and to check if they can cause knocking.

6.2.2.1. Parameter values justification

The range of different compression ratio values to be simulated is presented in Table 15, based on those considered in section 4.2.2.

Table 15 Range of compression values to be simulated

r_C to simulate	New gasket thickness (mm)	Clearance height (mm)
10.13	6.5	13.15
10.89	5.5	12.15
11.77	4.5	11.15
12.83	3.5	10.15
8.00	10.5	17.15

Values from Table 15 are selected to cover the range from 10.13 (the initially selected value – see sections 4.2.2 and 5.3.1) and 13 (the maximum recommended by the literature), in order to investigate the possibilities of a compression ratio increase. Additionally, it is simulated a much lower compression value (CR=8) than the initially selected.

6.2.2.2. Output data

Figure 31 shows the knocking probability for the whole range of simulated speeds and each value of the studied compression ratios. As seen, it is not expected to suffer knocking phenomenon for the initially selected CR value of 10.13. Besides, when increasing the CR value, the engine is still resistant to knocking for the range of simulated speeds. Also, when lowering this value to CR=8 knocking phenomenon does not occur as expected for lower compression ratios.

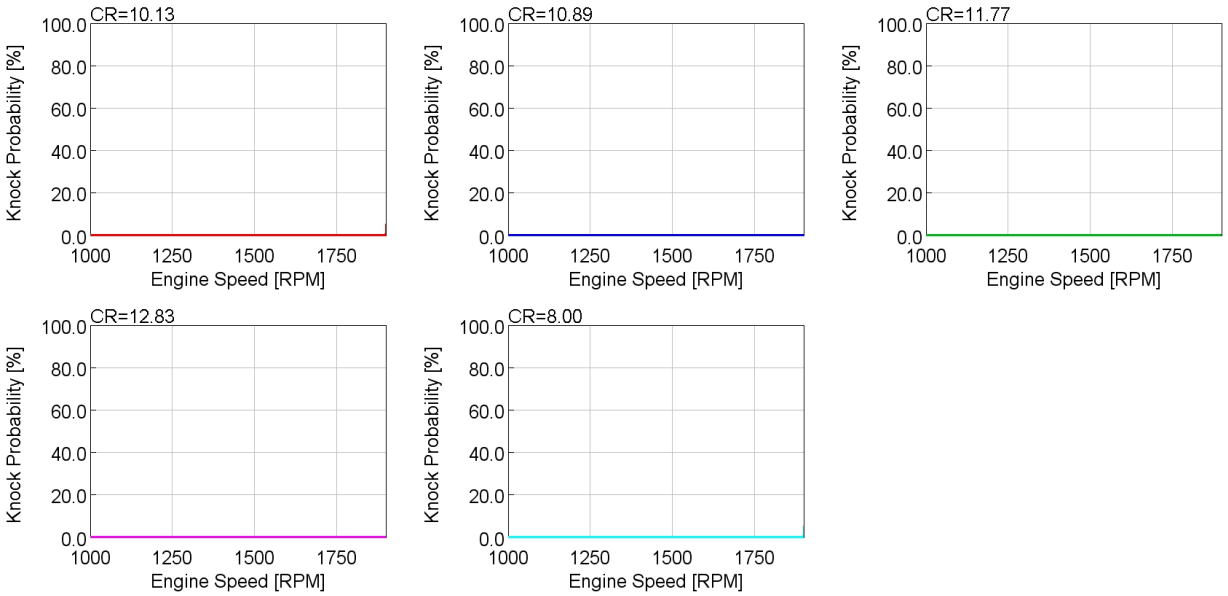

Figure 31 Knocking Probability for different compression ratios of the gas engine

Focusing on Figure 32 and Figure 33, it is analysed the effect of varying the compression ratio on engine performance.

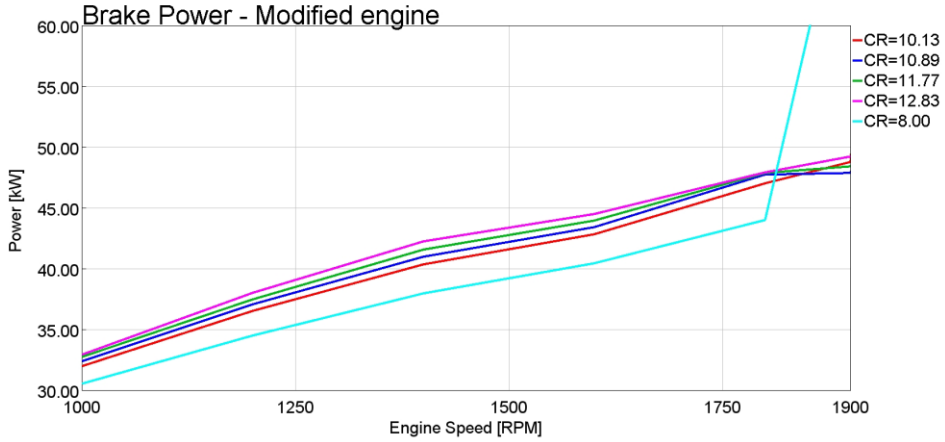

Figure 32 Effect of the compression ratio on the Brake Power curve of the gas engine

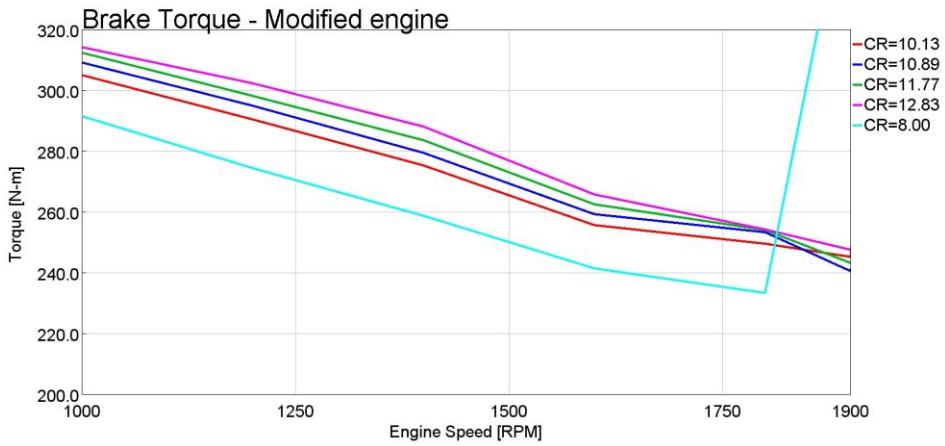

Figure 33 Effect of the compression ratio on the Brake Torque curves of the gas engine

Results show that rising the compression ratio derivates, in general lines, in better engine performance, as both power (Figure 32) and torque (Figure 33) increase. And this increase is more pronounced at mid speeds. If comparing the initially selected value for compression ratio (CR=10.13) and the highest simulated value (CR=12.83) it is appreciated an increase of 4.6% for both power and torque at 1400 rpm while at 1800 rpm this increase is only 2%.

Finally, in Figure 34 the effect of variating the CR on the Brake Specific Fuel Consumption (BSFC) is presented.

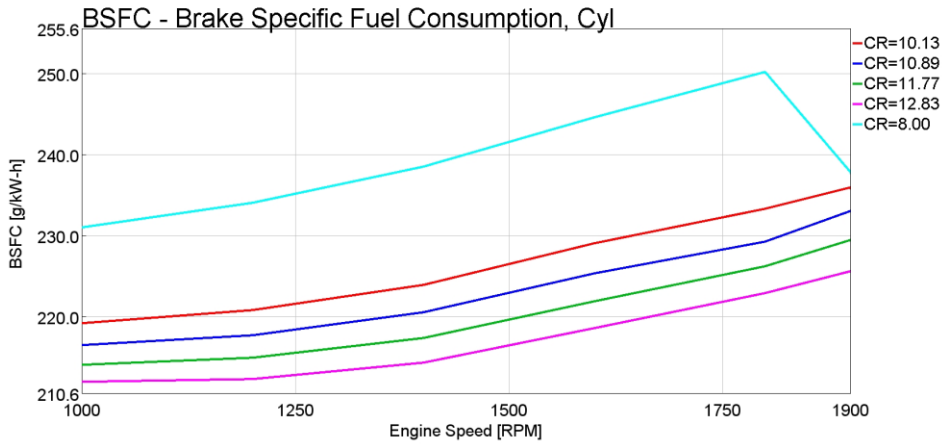

Figure 34 Effect of the compression ratio on the fuel consumption of the gas engine

The results from Figure 34 show that the BSFC is higher with lower compression ratio values. So, an increase from the initially selected CR (CR=10.13) to the maximum CR (CR=12.83), would imply a 4.5% decrease in the BSFC at 1800 rpm. At the same time, it shows that reducing the compression ratio to a low value such as 8 would result in a significant BSFC increase.

Therefore, these results reflect the possibility to optimise the engine performance by increasing the compression ratio to a value near 13 as suggested by the literature (section 3.3.1). The highest simulated value (RC=12.83) has shown better engine performance as well as lower BSFC while being resistant to knocking.

6.2.3. A/F ratio values sweep

The 17.2 initial CNG stoichiometric AFR value will undertake some variations to examine its influence on the gas engine performance and consumption. As stated in section 6.2.1, it will be swept the engine speed from 1000 to 1900 rpm.

6.2.3.1. Parameter values justification

From the stoichiometric CNG AFR, it will be taken two values above and two values below within a maximum range of about 10% difference since according to the literature (see section 4.2.3) the stoichiometric ratio should be the most appropriate. Table 16 are presented the AFR values to be simulated.

Table 16 Range of AFR values and their percentage difference to the stoichiometric value to be simulated

AFR	Percentage difference
19	+ 10.5 %
18	+ 4.7 %
17.2*	-
16	- 7 %
15	- 12.8 %

* Stoichiometric value used in the main simulation

6.2.3.2. Output data

As can be appreciated in Figure 35, all fuel ratios imposed when simulating are fulfilled which is a great indication to believe that the simulation has succeeded.

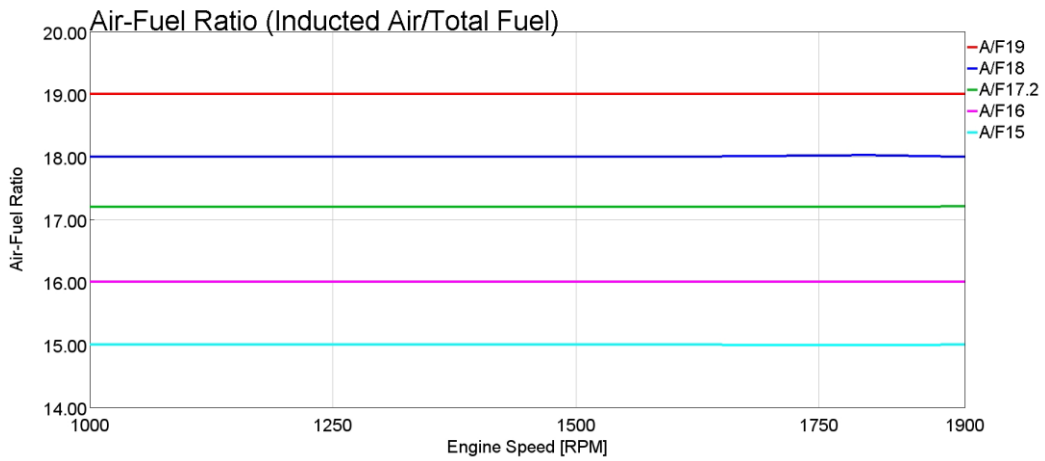

Figure 35 AFR of each case simulated of the gas engine

Figure 36 shows the effect of each AFR on the power curve while Figure 37 shows the effect of the AFR on the torque curve. Both charts demonstrate that the AFR above the stoichiometric – which is 17.2 – has a lower engine performance in terms of both power and torque than the stoichiometric one. For instance, the maximum percentage decrease between the AFR curve of 19 and the stoichiometric one is 13.7% both in terms of power and torque.

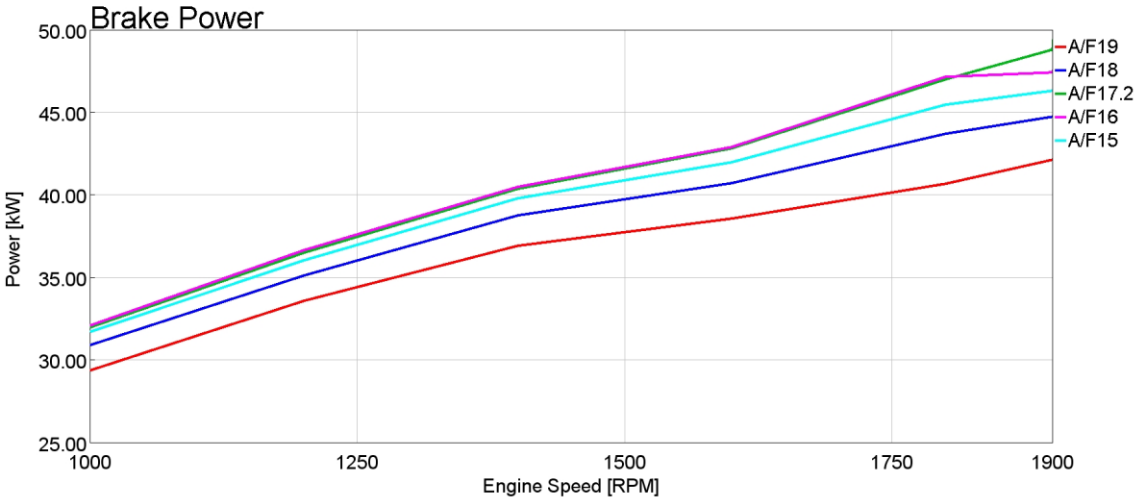

Figure 36 Effect of the AFR on the Brake Power curves of the gas engine

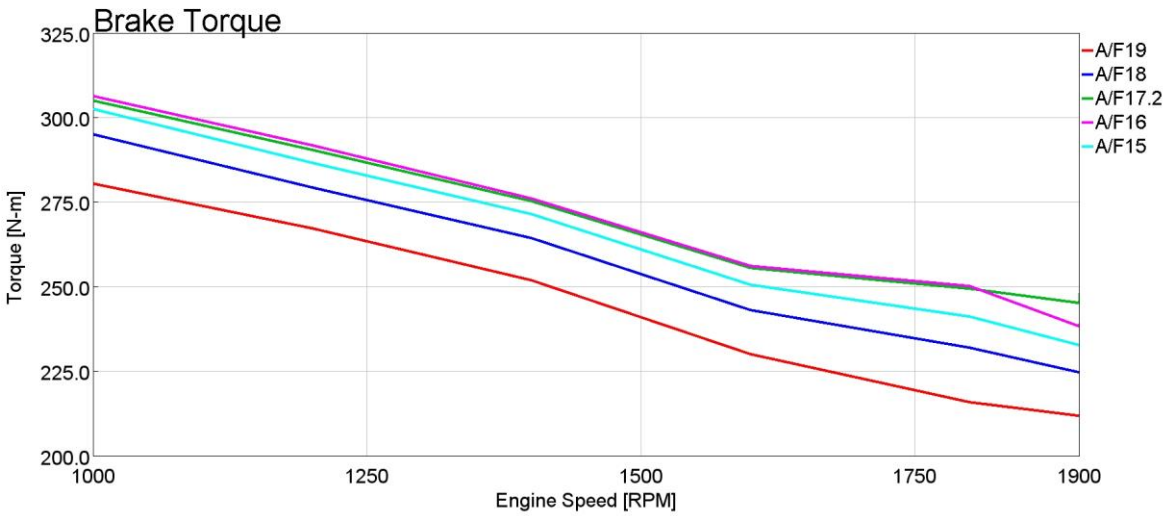

Figure 37 Effect of the AFR on the torque curves of the modified gas engine

However, according to Figure 36 and Figure 37 and focusing on AFR of 15 and 16 which are below the stoichiometric one, the engine performance is quite similar to the stoichiometric. Especially notice that the curves of the value 16 AFR have almost the same shape as the stoichiometric AFR curves. Therefore, it can be stated that within the range of AFR between 16-17.2 the engine performance can be considered identical so, theoretically, either value can be chosen arbitrarily when implementing the gas engine.

Finally, a comparison of engine consumption is to be undertaken. Figure 38 illustrates the Fuel Energy Entering Cylinder, Figure 39 shows the Throttle Angle, Figure 40 points out the Brake Specific Fuel Consumption (BSFC).

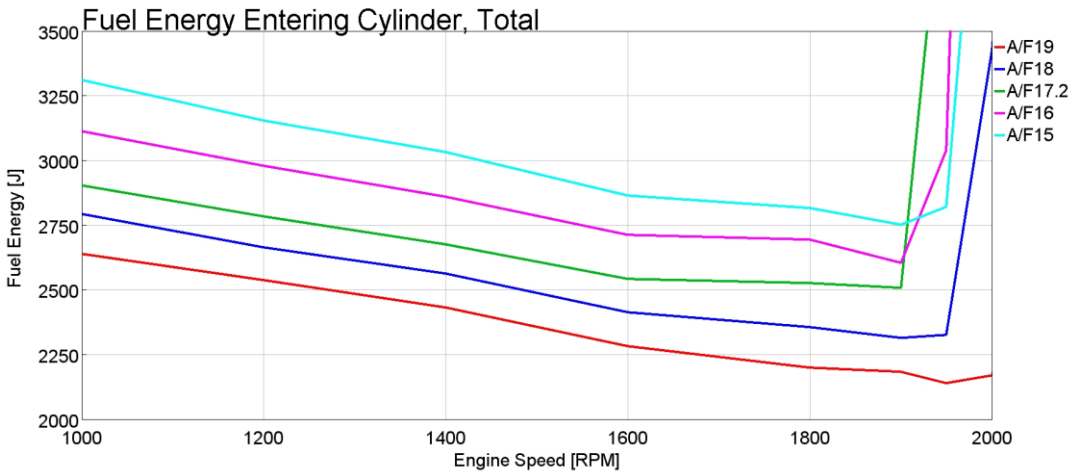

Figure 38 Effect of the AFR on the Fuel Energy Entering Cylinder curves of the gas engine

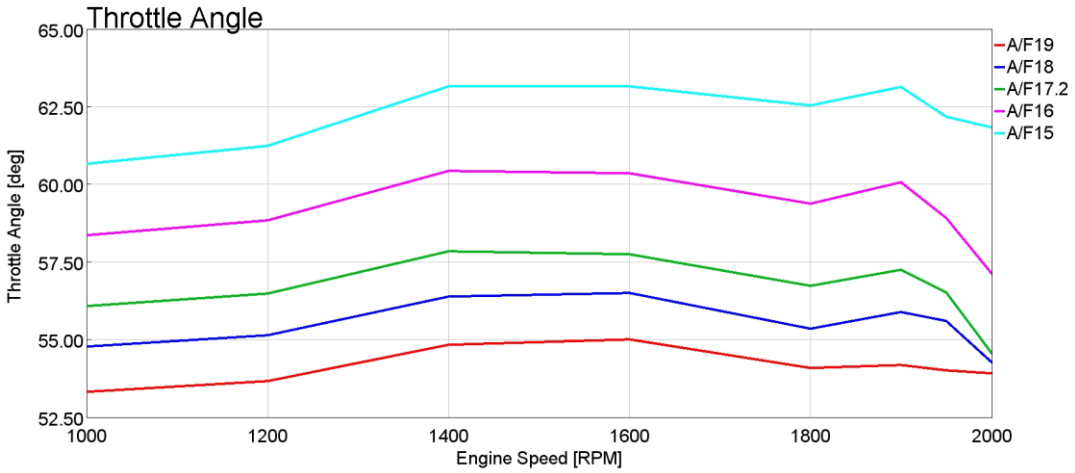

Figure 39 Effect of the AFR on the Throttle Angle curves of the gas engine

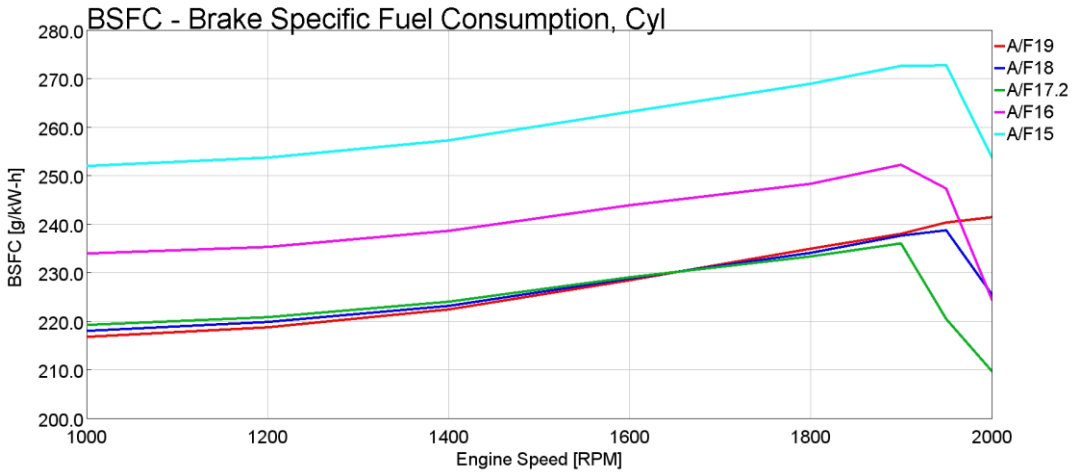

Figure 40 Effect of the AFR on the Brake Specific Fuel Consumption curves of the gas engine

About the Fuel Energy Entering Cylinder chart (Figure 38), it can be stated that the higher the AFR, the less energy enters the cylinder. This fact is logical since at a high AFR the mixture has a low proportion of CNG which means lower energy. As can be proved in Appendix IV, the real Sisudiesel engine has always 3870 J of fuel energy entering the cylinder since as stated in section 5.2.1, 90 mg of diesel is injected in every cycle. Therefore, according to the Figure 38 chart, setting an AFR close to the stoichiometric the fuel entering the cylinder is always lower in the CNG engine than in the real Sisudiesel engine.

Focusing on the Throttle Angle chart (Figure 39), the results can be considered consistent since at a lower AFR more fuel needs to be used so the throttle angle is to be higher. Finally, concentrating on the BSFC chart (Figure 40), AFR below the stoichiometric has a much higher brake specific fuel consumption than the stoichiometric and those above it. There is a maximum increase of 21% between the BSFC of the stoichiometric AFR and the AFR of 15. However, the AFRs above the stoichiometric one has a fuel consumption that can be considered almost identical to the stoichiometric. Notice that the gas engine BSFC range is between 210-275 g/kWh while according to Appendix IV the simulated Sisudiesel engine has a BSFC range between 250-330 g/kWh. Therefore, it can be stated that the gas engine is to be more efficient than the Sisudiesel engine.

Therefore, it can be concluded that the gas engine performance less power and torque and has lower fuel consumption than the actual Sisudiesel engine. The best AFR to be fixed in the gas engine is the stoichiometric one because the above AFRs have less engine performance and the below AFRs have higher consumption. That fact matches with the literature that suggests establishing a stoichiometric AFR.

7. Results and discussion

Initial aims and objectives

The first objective of the current thesis was to study the laboratory diesel engine described in section 3.1.2 and explore how can it be restructured to work on fuel gas. The engine has been analysed and well defined by consulting its manuals and by carrying out technical visits to the lab.

The following objective aimed to decide which was the most viable fuel gas to implement on the engine. This objective was met in section 3.2, conducting a literature review of the available gaseous fuels which includes diverse aspects such as their properties or their compatibility with the engine object of the study.

The third objective was to define the engine concept to be adapted for operating on fuel gas. Once the fuel gas was defined, Chapter 4 has proposed different engine modifying strategies supported by the previous literature review. The objective has been met by defining, in section 4.2, the strategy to be implemented based on the prior conducted study of the laboratory engine.

The last objective was intended to model and simulate the defined gas engine concept. This simulation has been successfully conducted using GT-Power software, allowing to check engine operation, performance, and consumption.

Other published work

Compared to other related work, this research had to deal with the fact that the Sisudiesel engine object of study is an old engine, which does not equip an electronic control unit (ECU). This has conditioned the adopted solutions for converting the engine to work on gas. In that respect, other authors opted for more contemporary solutions, for instance using gas fuel injectors electronically controlled (Kumar, 2018; Krishna, 2018) instead of the Venturi mixer. Besides, this investigation proposes to use of a fully mechanical ignition system, which since the end of the 1990s is not frequently used as stated by Reif (2015). But this does not make these adopted solutions less valid as they are simple and well-proven technology.

Regarding the performance decrease found when operating the engine on gas this investigation coincides with other authors. Simulation in section 6.2.1 showed a maximum 35% power decrease, similar to the 31.8% decrease observed by Chandra, et al. (2011). Also, less torque has been observed as in the case of Semin, et al. (2009b).

Limitations

There have been found some limitations to exactly reproduce the existing Sisudiesel engine in the modelling software. The model requires numerous detailed parameters, and it was possible to obtain some of them neither from the manufacturer data nor from laboratory measurements. This includes, for instance, some pipe dimensions in the intake manifold or a detailed intercooler. Thus, these values had to be estimated based mainly on the GT-Power bank of data.

Another example of this is the difficulties in modelling the engine turbocharger. The turbocharger of the Sisudiesel simulation is from a 6-cylinder engine. As explained in section 5.2.2 it was the only available turbocharger map data to implement. In comparison with the real Sisudiesel turbocharger, the 6-cylinder one has less speed but more mass flow rate and pressure ratio (according to compressor data from BorgWarner (n.d.)). It is one of the main reasons why the simulation output is not exactly the same as the Sisudiesel data. Attempts have been made to contact manufactures to get the data without success. Nevertheless, after all, it does not affect the aim of the work since the same turbocharger is implemented in the real Sisudiesel and the modified one so a sensitivity analysis can be performed with no problems.

Consistencies and inconsistences

The investigation has achieved a valid gas engine concept and a simple modifying strategy, suitable for the Sisudiesel considering its characteristics. The engine simulation shows logical results in the engine range of speeds between 1000 and about 2000 rpm. But it is from this speed that the simulations results are inconsistent. This might be attributed, on one hand, to the described modelling limitations and on the other hand, to the fact that the original diesel engine

is designed to operate at low speeds. A speed exceed would imply inertial problems since according to the engine dimensions is to run at a maximum of 2200 rpm (see Appendix III).

8. Conclusion

Alternatives fuels such as fuel gases are a mid-term alternative for IC engines to reduce their emissions. Thus, it is worthwhile for the Novia UAS engine laboratory to have a gas engine. Research has been conducted to decide the most appropriate fuel gas to implement and the most feasible strategy to adapt the engine. In that respect, it has been found that there are multiple valid options to adapt the diesel engine, with its benefits and drawbacks. Moreover, an adequate fuel gas has been chosen and an engine concept presented in agreement with the project scope.

It has been determined that CNG is the most appropriate fuel gas to implement in the engine. Principally because of the engine implementation feasibility but also according to its availability and ease of storage. Then, it has been presented the chosen engine concept to operate on CNG, which consist of a spark-ignition engine with a Venturi mixer as the main part of the fuel system and a reduced compression ratio regarding the initial diesel engine to avoid the knocking phenomenon.

The modelling and simulation of the defined engine concept have allowed checking the appropriate engine operation and its performance. According to the simulation results, the modified engine has an adequate operation at low engine speeds (1000 to 2000 rpm). But at higher speeds, it has not been possible to obtain consistent simulation results. Besides, in the range of the consistent results, it has been found that the gas engine has a lower performance compared to that of the original diesel engine. Specifically, the gas engine has 10-35% less power and 12-33% less torque than the Sisudiesel which is in line with the literature.

The simulation has also taken the first approach to optimize the CR value. It has shown that by increasing CR from the lowest values suggested by the literature (8-10) to values around 13, the engine performance and efficiency slightly improve while maintaining it within the knocking limits. Regarding the optimization of the CNG AFR, it has been possible to demonstrate through the simulation that, as stated in the literature, the best option is to keep the stoichiometric ratio, which is exactly 17.2. Maintaining the stoichiometric ratio improves engine performance as well as enhances CNG consumption.

Therefore, it can be concluded that the thesis has been successfully developed and that all the proposed objectives within the scope of the research have been achieved.

With regards to recommendations and suggestions for future research, this thesis can be considered the first step in the aim of having a gas engine in the lab for academic applications. It has been undertaken theoretical research about the best fuel gas and the optimal strategy to carry out the engine modifications, all supported by simulations in the GT-Power. Thus, plenty of future research could benefit from this thesis' conclusions which can be divided into two parts. On the one hand, improving the GT-Power simulations considering additional data. On the other hand, carrying out the physical implementation of the engine in the lab.

Below, the most important insights for future research are presented.

GT-Power simulations

- Disassemble the existing lab engine to be able to measure in detail all the engine parts and input that data into GT-Power to obtain a simulation even closer to reality – especially measure the pipes of the intake and exhaust manifold.
- Collect lab data from the real Sisudiesel turbocharger and implement it in GT-Power – including the by-pass to have a simulation closer to reality.
- Research a gas turbocharger map to implement and improve the gas engine performance.

PHYSICAL IMPLEMENTATION

- Design and manufacture the head spacer
- Design the ignition system or adapt an existing one
- Benchmark catalogues from manufactures to acquire the proper parts to work in a gas engine such as the gas mixer, spark plugs… taking into account both economic aspects and optimum engine performance
- Design the exhaust gas treatment system
- Implement physically the engine gas in the lab

9. References

Agco Power, 2020. *Agcopower.* [Online]
Available at: https://www.agcopower.com/
[Accessed 10 Mar. 2021].

Aina, T., Folayan, C. O. & Pam, G. Y., 2012. Influence of compression ratio on the performance characteristics of a spark ignition engines. *Advances in Applied Science Research,* 3(4), pp. 1915-1922 .

Ashok, B., Denis, S. & Ramesh, C., 2015. LPG diesel dual fuel engine - A critical review. *Alexandria Engineering Journal,* 54(2), pp. 105-126.

Bari, S. & Hossain, N., 2018. *Performance of a diesel engine run on diesel and natural gas in dual-fuel mode of operation,* Sydney: Elsevier.

Bari, S. & Hossain, N., 2019. Performance of a diesel engine run on diesel and natural gas in dual-fuel mode of operation. *Energy Procedia,* Volume 160, pp. 215-222.

Baumgärtner, F. & Letmathe, P., 2020. External costs of the Dieselgate – Peccadillo or substantial consequences?. *Transportation Research Part D: Transport and Environment,* Volume 87.

Bioenergia, 2021. *Tilastot ja julkaisut – Bioenergia ry.* [Online]
Available at: https://www.bioenergia.fi/tietopankki/tilastot-ja-julkaisut/
[Accessed 20 Apr. 2021].

BorgWarner, n.d. *S1B 100-180 HP,* s.l.: s.n.

Bsuplemen, 2021. *High Impedance Fuel Injector for Bosch as Petrol methanol.* [Online]
Available at:
https://www.bsuplemen.com/index.php?main_page=product_info&products_id=614718
[Accessed 6 May 2021].

Çengel, Y. A. & Boles, M. A., 2014. *Thermodynamics. An engineering.* 8th ed. New York: McGraw-Hill Education.

Chala, G. T., Abd Aziz, A. R. & Hagos, F. Y., 2018. Natural Gas Engine Technologies: Challenges and Energy Sustainability Issue. *Energies,* 11(11).

Chandra, R., Vijay, V., Subbarao, P. & Khura, T., 2011. Performance evaluation of a constant speed IC engine on CNG, methane enriched biogas and biogas. *Applied Energy,* 88(11), pp. 3969-3977.

Cummins Westport, 2018. *Fuel Quality Calculator.* [Online]
Available at: https://www.cumminswestport.com/fuel-quality-calculator
[Accessed 5 May 2021].

European Committee for Standardization, 2009. *Automotive fuels - diesel - Requirements and test methods - EN 590:2009:en,* Brussels: CEN.

Finnish Standards Association, 2017a. *Natural gas and biomethane for use in transport and biomethane for injection in the natural gas network. Part 2: Automotive fuels specification - SFS-EN 16723-2:2017:en,* Finland: SFS.

Finnish Standards Association, 2017b. *Natural gas. Vocabulary - SFS-EN ISO 14532:2017:en,* Finland: SFS Online.

Fox Venturi Products, 2020. *Naval and Marine Applications.* [Online]
Available at: https://www.foxvalve.com/liquid-eductors/naval-and-marine-applications/
[Accessed 7 May 2021].

Frangoul, A., 2021. *Volvo says it will be 'fully electric' by 2030 and move car sales online.* [Online]
Available at: https://www.cnbc.com/2021/03/02/volvo-says-it-will-be-fully-electric-by-2030-move-car-sales-online.html
[Accessed 2 May 2021].

Gamma Technologies, 2020. *GT-Suite, Engine Performance Tutorials,* s.l.: s.n.

Gamma Technologies, 2021. *GTISOFT.* [Online]
Available at: https://www.gtisoft.com/
[Accessed 25 Apr. 2021].

Gardiner, D., Bardon, M. & Pucher, G., 2008. *An Experimental and Modeling Study of the Flammability of Fuel Tank Headspace Vapors from High Ethanol Content Fuels,* Golden: National Renewable Energy Laboratory.

Gasgrid, 2021. *What is flowing in our pipelines?.* [Online]
Available at: https://gasgrid.fi/en/gas-network/what-is-flowing-in-our-pipelines/
[Accessed 25 Apr. 2021].

Gasum, 2021a. *Gas filling stations.* [Online]
Available at: https://www.gasum.com/en/sustainable-transport/road-transport/Gas-filling-stations/
[Accessed 1 Apr. 2021].

Gasum, 2021b. *Tankkaa kaasua.* [Online]
Available at: https://www.gasum.com/yksityisille/tankkaa-kaasua/tankkausasemat/
[Accessed 1 Apr. 2021].

Gasum, 2021c. *Gasum biogas plants in Nordics.* [Online]
Available at: https://www.gasum.com/en/our-operations/biogas-production/biogas-plants/
[Accessed 20 Apr. 2021].

Ghosh, A., 2020. Possibilities and Challenges for the Inclusion of the Electric Vehicle (EV) to Reduce the Carbon Footprint in the Transport Sector: A Review. *Energies,* Volume 12, p. 2602.

Gnanamoorthia, V. & Devaradjaneb, G., 2015. Effect of compression ratio on the performance, combustion and emission of DI diesel engine fueled with ethanol – Diesel blend. *Journal of the Energy Institute,* 88(1), pp. 19-26.

Go With Natural Gas, 2014. *Natural Gas as a Vehicle Fuel - CNG & LNG.* [Online]
Available at: https://cngva.org/wp-content/uploads/2017/12/CNG-LNG-Factsheet-FINAL-EN.pdf
[Accessed 20 Feb. 2021].

Grzywacz, R., 2017. *The mixing hydrodynamics and efficiency of the venturi jet,* Cracow: Department of Chemical and Process Engineering, Faculty of Chemical Engineering and Technology, Cracow University of Technology.

IEA, 2020. *Outlook for biogas and biomethane: Prospects for organic growth,* Paris: IEA.

Imran Khan, M., Yasmin, T. & Shakoor, A., 2015. Technical overview of compressed natural gas (CNG) as a transportation fuel. *Renewable and Sustainable Energy Reviews,* Volume 51, pp. 785-797.

Klaus von Mitzlaff, 1988. *Engines for biogas.* Eschborn: Deutsche Gesellschaft für Technische Zusammenarbeit (GTZ) GmbH.

Kok, J. & van der Wal, S., 1996. Mixing in T-junctions. *Applied Mathematical Modelling,* 20(3), pp. Mixing in T-junctions.

Krishna, R. S., 2018. Conversion of Diesel engine to CNG engine of commercial vehicle and emission control. *International Journal of Mechanical and Production Engineering,* 6(11), pp. 30-35.

Kumar, G., 2018. *Conversion of Diesel Engine to CNG Engine,* s.l.: s.n.

Malenshek, M. & Olsen, D. B., 2009. Methane number testing of alternative gaseous fuels. *Fuel,* 88(4), pp. 650-656.

Mohamad, T. I., 2006. *Development of a spark plug fuel injector for direct injection of natural gas in spark ignition engine,* s.l.: s.n.

Mohamad, T. I., 2010. Compressed Natural Gas Direct Injection (Spark Plug Fuel Injector). In: P. Potocnik, ed. *Natural Gas.* Rijeka: SCIYO, pp. 289-306.

Motortech, 2018. *VariFuel2/VariFuel2+ - Motortech Air/Gas Mixer.* s.l.:s.n.

NGK, 2019. *LPG LaserLine - the best for gas powered engines,* s.l.: NGK.

Porssitieto, 2021. *Keräilijäin Osakekirjat.* [Online]
Available at: www.porssitieto.fi/osake/lists.html
[Accessed 10 Mar. 2021].

Prasad, R. K., Kar, T. & Agarwal, A. K., 2019. Prospects and Challenges for Deploying Direct Injection Technology for Compressed Natural Gas Engines. In: K. K. Srinivasan, A. K. Agarwal, S. R. Krishnan & V. Mulone, eds. *Natural Gas Engines.* Singapore: Springer Singapore, pp. 117-141.

Ramadhas, A. S. ed., 2011. *Alternative Fuels for Transportation.* s.l.:Taylor & Francis Group.

Reif, K., ed., 2014. *Diesel Engine Management.* 1 ed. Wiesbaden: Springer Vieweg.

Reif, K., ed., 2015. *Gasoline Engine Management.* 1 ed. Friedrichshafen: Springer Vieweg.

Reitz, R. et al., 2020. IJER editorial: The future of the internal combustion engine. *International Journal of Engine Research,* 21(1), pp. 3-10.

Rodriguez Cussó, R., 2013. *Análisis y adaptación de motores de ciclo Otto y Diesel operando con biogás,* Barcelona: s.n.

Ryckebosch, E., Drouillon, M. & Vervaeren, H., 2011. Techniques for transformation of biogas to biomethane. *Biomass and Bioenergy,* 35(5), pp. 1633-1645.

Salles, Q. et al., 2019. *Fuel For the Future - European Project Semester,* Vaasa: Novia University of Applied Science.

Sandfirden Technics, 2020. *About Sandfirden Technics.* [Online]
Available at: https://www.sandfirden.nl/en/company-info/
[Accessed 27 Apr. 2021].

Sandfirden Technics, n.d. *Industrial Gas Engine SGI-4.* Den Oever: Sandfirden Technics.

Scania, 2018. *Scania engines being tested with raw untreated biogas.* [Online]
Available at: https://www.scania.com/group/en/home/newsroom/news/2018/scania-engines-

being-tested-with-raw-untreated-biogas.html
[Accessed 3 Apr. 2021].

Schobert, H. H., 2014. *Energy and society.* Second ed. s.l.:CRC Press.

Semin, Bakar, R. A. & Ismail, A. R., 2009a. Green Engines Development Using Compressed Natural Gas as an Alternative Fuel: A Review. *American Journal of Environmental Sciences,* 5(3), pp. 371-381.

Semin, Ismail, A. R. & Abu, B. R., 2009b. Investigation of Torque Performance Effect on the Development of Sequential Injection CNG Engine. *Journal of Applied Sciences,* 9(13), pp. 2416-2423.

Semin, Ismail, A. R. & Bakar, R. A., 2009c. Diesel Engine Convert to Port Injection CNG Engine Using Gaseous Injector Nozzle Multi Holes Geometries Improvement: A Review. *American J. of Engineering and Applied Sciences,* 2(2), pp. 268-278.

Serrano, J. R., Novella, R. & Piqueras, P., 2019. Why the Development of Internal Combustion Engines Is Still Necessary to Fight against Global Climate Change from the Perspective of Transport. *Applied Sciences,* 9(21), p. 4597.

Shimatsu, T., 2017. *Development of Bi-Fuel Systems for Satisfying CNG Fuel Properties,* s.l.: s.n.

Shinde, T. B., 2012. Experimental investigation on effect of combustion chamber geometry and port fuel injection system for CNG engine. *IOSR Journal of Engineering,* 2(7), pp. 49-54.

Siripornakarachai, S. & Sucharitakul, T., 2007. Modification and tuning of diesel bus engine for biogas electricity production. *Maejo International Journal of Science and Technology,* 1(2), pp. 194-207.

Sisu Diesel Inc., 2002. *Workshop Manual 320 420 650 634.* Nokia: Sisu Diesel Inc..

Sparex, 2021. *Head Gasket - 4 Cyl. (420D, 420DS, 420DR, 420DRS, 420DW, 420DSI, 420DS).* [Online]
Available at: https://gb.sparex.com/head-gasket-4-cyl-420d-420ds-420dr-420drs-420dw-420dsi-420ds-110945.html
[Accessed 7 May 2021].

Speight, J. G., 2015. Handbook of Alternative Fuel Technologies (second ed.). In: S. Lee, J. G. Speight & S. K. Loyalka, eds. *Alternative Fuel Technologies.* Boca Raton: Taylor & Francis Group, LLC, pp. 157-178.

Stanadyne, 2007. *Cross Reference Guide for Injector, Nozzle Assembly, PF Pump and Pencil Nozzle,* USA: s.n.

Statista, 2020. *The Statistics Portal.* [Online]
Available at: https://www.statista.com/search/?q=agco&Search=&qKat=search
[Accessed 27 Apr. 2021].

Stone, R., 2012. *Introduction to internal combustion engines.* 4th ed. New York: Palgrave Macmillan.

STORMOSSEN, 2021. *Info about biogas.* [Online]
Available at: https://www.stormossen.fi/en/info-about-biogas/
[Accessed 1 Apr. 2021].

Teboil, 2020. *Teboil LPG.* [Online]
Available at: https://www.teboil.fi/en/products/teboil-lpg/
[Accessed 25 Apr. 2021].

Wappelhorst, S., 2020. *The end of the road? An overview of combustion engine car phase-out announcements across Europe.* [Online]
Available at: https://theicct.org/sites/default/files/publications/Combustion-engine-phase-out-briefing-may11.2020.pdf
[Accessed 2 May 2021].

Wayan Surata, I. et al., 2014. Simple Conversion Method from Gasoline to Biogas Fueled Small Engine to Powered Electric Generator. *Energy Procedia,* Volume 52, pp. 626-632.

Wellinger, A. & Lindberg, A., 2005. *Biogas Upgrading and Utilisation,* s.l.: IEA.

Winquist, E., Rikkonen, P., Pyysi€ainen, J. & Varho, V., 2019. Is biogas an energy or a sustainability product? - Business opportunities in the Finnish biogas branch. *Journal of Cleaner Production,* Volume 233, pp. 1344-1354.

Xiang, L. et al., 2020. Parametric Knocking Performance Investigation of Spark Ignition Natural Gas Engines and Dual Fuel Engines. *Journal of Marine Science and Engineering,* Volume 8, p. 459.

Appendix I. Calculations

1. Compression ratio and gasket thickness

The compression ratio (r_C) is defined as:

$$r_C = \frac{V_D + V_C}{V_C} \quad (1)$$

Where:

V_D Displacement volume
V_C Clearance volume

And clearance volume (V_C) is defined as:

$$V_C = \pi \frac{D^2}{4} \cdot h_C \quad (2)$$

Where:

D Cylinder bore
h_C TDC Clearance Height

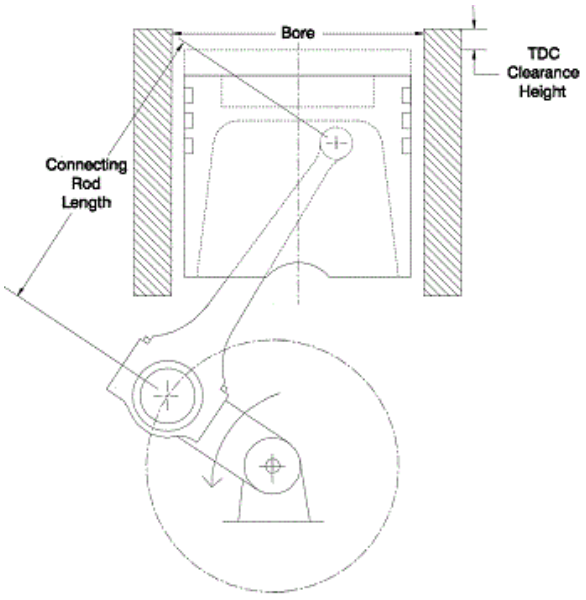

Generic cylinder drawing, with the TDC Clearance Height parameter represented – adapted from Gamma Technologies (2021)

1.1. Original engine clearance height

From the Sisudiesel 420 DWRIE engine manual (Sisu Diesel Inc., 2002), the following data is obtained.

Compression ratio	$r_C = 16.5$
Cylinder bore (mm)	$D = 108$
Cylinder displacement volume (mm^3)	$V_D = 1{,}1$

From this data and using formulas (1) and (2), the original engine h_C is obtained:

$$h_C = \frac{4 \cdot V_D}{\pi \cdot D^2 \cdot (r_C - 1)} = 7{,}75 \text{ mm}$$

1.2. Modified clearance height and compression ratio

The replacement of the cylinder head gasket modifies the original clearance height (h_C). Be d_1 the thickness of the existing cylinder head gasket, and d_2 the thickness of the new cylinder head gasket. Then, and according to formulas (1) and (2), the new clearance height ($h_C{}'$) is defined as:

$$h_C{}' = h_C + d_2 - d_1 \qquad (3)$$

Thus, the new compression ratio ($r_C{}'$) is defined:

$$r_C{}' = \frac{4 \cdot V_D}{\pi \cdot D^2 \cdot h_C{}'} + 1 \qquad (4)$$

2. Injected mass

The Sisudiesel 420 DWRIE engine manual (Sisu Diesel Inc., 2002, pp. 14-5) gives the data of the pumped fuel per stroke:

$$V_f = 107\ \text{mm}^3/\text{stroke}$$

From this value, it can be calculated the total fuel injected mass ($m_{f,total}$) in one engine cycle:

$$m_{f,total} = V_f \cdot 4\ \text{strokes}\ \cdot \rho_{fuel} \qquad (5)$$

Where:

V_f Fuel volume per stroke
ρ_{fuel} Fuel density

So, the total fuel injected mass ($m_{f,total}$) in one engine cycle is:

$$m_{f,total} = 107\ \frac{\text{mm}^3}{\text{stroke}} \cdot 4\ \text{strokes}\ \cdot 848 \cdot 10^{-3}\ \frac{\text{mg}}{\text{mm}^3} = 362.94\ \text{mg}$$

As there are four injectors, the injected mass (m_f) on each one is:

$$m_f = \frac{362.94}{4} \approx 90\ \text{mg}$$

Appendix II. GT-Power simulation data

This appendix summarizes a set of data that has been inputted in GT-Power simulation software.

Basic simulation parameters

The following table shows the parameters that have been introduced to GT-Power simulation software. In the column called *Modified gas engine model,* only those items that differ between the Sisudiesel engine model and the modified engine model are specified. The blank cells indicate that there are no changes in the modified gas engine model compared to the diesel engine model.

	Description	GT-Power Template	Part Name	Properties	Unit	Sisudiesel 420 DWRIE model	Modified gas engine model
	1.1. Intake Port and Runner	PipeRound	intrunner	Diameter at Inlet End	mm	48	
				Length	mm	120	
				Discretization Length	mm	40	
				Initial State Name		initial	intake_initial
				Roughness from Material		cast_iron	
				Wall Layer Properties Object		inlet	
				Wall External Boundary Conditions Objec		inletWallLayer	
				Initial Wall Temperature	K	350	
		PipeRound	intport	Diameter at Inlet End	mm	48	
				Diameter at Outlet End	mm	def	
				Length	mm	80	
				Discretization Length	mm	40	
				Initial State Name		initial	intake_initial
				Rougness from Material		cast_iron	
				Impossed wall Temperature	K	450	
				Heat transfer Multiplier		1,5	
				Heat Input Rate	W	ign	
				Thermocouple Object		ign	
				No Friction Pressure Losses		true	
				Zero Pressure Losses from Bands and Tap		true	
	1.2. Intake and exhaust valves	ValveCamConn	intvalve	Cam Timin Angle	Cam Angle	458	
				Valve Lash	mm	0,1	
				Angle Multiplier		1	
				Anchor for Angle Multiplier		Theta=0	
				Lift Multiplier		1	
				Valve Reference Diameter		48	
				Discharge Coefficient Reference Area Def		constant	
				Flow Coefficient Lift Unit		LiftOverDiam	
				Flow Area Multiplier		1	
				Number of Identical Holes		def	
				Cam Timin Angle	Cam Angle	251	
				Valve Lash	mm	0,1	
				Angle Multiplier		1	
				Anchor for Angle Multiplier		Theta=0	

1. Basic engine		ValveCamConn	exhvalve	Lift Multiplier		1	
				Valve Reference Diameter	mm	41	
				Discharge Coefficient Reference Area Def		constant	
				Flow Coefficient Lift Unit		LiftOverDiam	
				Flow Area Multiplier		1	
				Number of Identical Holes		def	
	1.3. Cylinder	EngCylinder	cylinder	Initial State Object		initial	intake_initial
				Wall Temperature defined by Reference C		twall	
				Heat Transfer Object		htr	
				Flow Object		ign	
				Combustion Object		comb	gas_Comb
				Measured Cylinder Pressure Analysis Obje		ign	
				Cylinder Pressure Analysis Mode		off	
	1.4. Fuel Injector	InjDieselSimpleConn	di-inject	Injected Mass	mg	90	deleted
				Fluid Object		diesel2-combust	deleted
				Injected Fluid Temperature	K	300	deleted
				Injection Timing	deg	1	deleted
				Injection Duration	deg	19	deleted
	1.5. Exhaust Port and Runner	PipeRound	exhport	Diameter at Inlet End	mm	41	
				Diameter at Outlet End	mm	def	
				Length	mm	60	
				Discretization Length	mm	55	
				Initial State Name		initial_exh	
				Roughness from Material		cast_iron	
				Imposed Wall Temperature	K	550	
				Heat Transfer Multiplier		1,5	
				Heat Input Rate	W	ign	
				Thermocouple Object		ign	
		PipeRound	exrunner	Diameter at Inlet End	mm	41	
				Diameter at Outlet End	mm	def	
				Length	mm	150	
				Discretization Length	mm	55	
				Initial State Name		initial_exh	
				Roughness from Material		steel	
				Imposed Wall Temperature	K	600	
				Heat Transfer Multiplier		def	
				Heat Input Rate	W	ign	
				Thermocouple Object		ign	
	1.7. Engine Crank Train	EngineCrankTrain	engine	Engine Type		4-stroke	
				Speed or Load Specification		speed	
				Engine Speed	RPM	[RPM]	
				Engine Friction Object or FMEP	bar	friction	
				Start of Cycle (CA at IVC)		-95	
				Cylinder Geometry Object		geom	
				Crank-Slider Inertia Object		ign	
				Cylinder Number		1-2-4-3	
				Firing Intervals		0-180-180-180	
				Cylinder Number		1	
				Firing Intervals	deg	0	
				Reference State for Volumetric Efficiency		initial	
				Part Name for Manifold Volumetric Eff. R		ign	
				RLT for Percent Load Calculation		ign	
				100% Load Table Name		ign	
		PipeRound	pipe-to-int	Diameter at Inlet End	mm	55	
				Diameter at Outlet End	mm	def	
				Length	mm	450	
				Discretization Length	mm	40	
				Initial State Name		initial	intake_initial
				Rougness from Material		cast_iron	
				Impossed wall Temperature		350	
				Heat Transfer Multiplier		def	
				Heat Input Rate		ign	
				Thermocouple Object		ign	
				Diameter at Inlet End	mm	55	
				Diameter at Outlet End	mm	70	
				Length	mm	40	
				Discretization Length	mm	40	

	2.1. Intercooler	PipeRound	cooler-in-1	Initial State Name		initial	intake_initial
				Roughness from Material		steel	
				Wall Layer Properties Object		inlet	
				Wall External Boundary Conditions Objec		inletWallLayer	
				Initial Wall Temperature	K	350	
			cooler-in-2	Diameter at Inlet End	mm	70	
				Length	mm	40	
				Discretization Length	mm	40	
				Initial State Name		initial	intake_initial
				Roughness from Material		steel	
				Wall Layer Properties Object		inlet	
				Wall External Boundary Conditions Objec		inletWallLayer	
				Initial Wall Temperature	K	350	
		FlowSplitGeneral	cooler-fsplit	Volume	mm^3	190000	
				Surface Area	mm^2	def	
				Initial State Name		initial	intake_initial
				Roughness from Material	steel	steel	
				Wall Layer Properties Object		inlet	
				Wall External Boundary Conditions Objec		inletWallLayer	
				Initial Wall Temperature	K	350	
				Link Name or Number		1-2	
				Angle (Planar Configuration)		0-180	
				Characteristic Length_1	mm	30	
				Characteristic Length_2	mm	30	
				Expansion Diameter_1	mm	90	
				Expansion Diameter_2	mm	90	
		PipeRound	cooler	Diameter at Inlet End	mm	7	
				Length	mm	300	
				Discretization Length	mm	40	
				Initial State Name		initial	intake_initial
				Roughness from Material		steel	
				Imposed Wall Temperature	K	350	
				Heat Transfer Multiplier		10	
				Friction Multipler		[friction]	
		OrificeConn	nocond	This orifice connection prevents conducti			
		IntercoolerEff	IC-Eff	Effectiveness Table or Function Object			
				Coolant Temperature	K		
		PipeRound	pipe-to-man	Diameter at Inlet End	mm	70	
				Length	mm	100	
				Discretization Length	mm	40	
				Initial State Name		initial	intake_initial
				Roughness from Material		steel	
				Wall Layer Properties Object		inlet	
				Wall External Boundary Conditions Objec		inletWallLayer	
				Initial Wall Temperature	K	350	
		FlowSplitGeneral	intmancool-fs	Volume	mm^3	700000	
				Surface Area	mm^2	def	
				Initial State Name		initial	intake_initial
				Roughness from Material	steel	cast_iron	
				Wall Layer Properties Object		InMan	
				Wall External Boundary Conditions Objec		InManWallLayer	
				Initial Wall Temperature	K	350	
				Link Name or Number		1-2-3	
				Angle (Planar Configuration)		0-180-(-90)	
				Characteristic Length_1	mm	70	
				Characteristic Length_2	mm	70	
				Characteristic Length_3	mm	70	
				Expansion Diameter_1	mm	112,84	
				Expansion Diameter_2	mm	112,84	
				Expansion Diameter_3	mm	157,98	
		PipeRectangle	ntmancool-pipe	Height at Inlet End	mm	100	
				Width at Inlet End	mm	100	
				Length	mm	8	
				Discretization Length	mm	40	
				Roughness from Material		cast-iron	
				Discretization Length	mm	40	
				Initial State Name		initial	intake_initial

d exhaust systems

2.2 Intake Manifold

2. Intake an	2.2 Intake Manifold			Roughness from Material		cast_iron	
				Wall Layer Properties Object		InMan	
				Wall External Boundary Conditions Objec		InManWallLayer	
				Initial Wall Temperature	K	350	
				Volume	mm^3	480000	
				Surface Area	mm^2	def	
				Initial State Name		initial	intake_initial
				Roughness from Material	steel	cast_iron	
				Wall Layer Properties Object		InMan	
				Wall External Boundary Conditions Objec		InManWallLayer	
				Initial Wall Temperature	K	350	
		FlowSplitGeneral	intman-fs	Link Name or Number		1-2-3	
				Angle (Planar Configuration)		0-180-90	
				Characteristic Length_1	mm	48	
				Characteristic Length_2	mm	48	
				Characteristic Length_3	mm	48	
				Expansion Diameter_1	mm	112,84	
				Expansion Diameter_2	mm	112,84	
				Expansion Diameter_3	mm	157,98	
				Height at Inlet End	mm	100	
				Width at Inlet End	mm	100	
				Length	mm	86	
				Discretization Length	mm	40	
		PipeRectangle	intman-pipe	Initial State Name		initial	intake_initial
				Roughness from Material		cast_iron	
				Wall Layer Properties Object		InMan	
				Wall External Boundary Conditions Objec		InManWallLayer	
				Initial Wall Temperature	K	350	
		OrificeConn	bellmouth	st pipe to ensure the environment pressur			
		EndFlowCap	def				
	2.3. Exhaust Manifold			Volume	mm^3	294000	
				Surface Area	mm^2	def	
				Initial State Name		initial_exh	
				Roughness from Material		steel	
				Imposed Wall Temperature	K	600	
				Link Name or Number		1-2-3	
		FlowSplitGeneral	exhman-fs	Angle (Planar Configuration)		0-180- (-90)	
				Characteristic Length_1	mm	60	
				Characteristic Length_2	mm	60	
				Characteristic Length_3	mm	60	
				Expansion Diameter_1	mm	78,99	
				Expansion Diameter_2	mm	78,99	
				Expansion Diameter_3	mm	110,589	
				Height at Inlet End	mm	70	
				Width at Inlet End	mm	70	
				Length	mm	77	
		PipeRectangle	exhman-pipe	Discretization Length	mm	60	
				Initial State Name		initial_exh	
				Roughness from Material		steel	
				Imposed Wall Temperature	K	600	
		EndFlowCap	def				
				Height at Inlet End	mm	70	
				Width at Inlet End	mm	70	
				Length	mm	27,6	
		PipeRectangle	exhmanturb-pip	Discretization Length	mm	60	
				Roughness from Material		steel	
				Initial State Name		initial_exh	
				Imposed Wall Temperature	K	600	
				Volume	mm^3	107065	
				Surface Area	mm^2	def	
				Initial State Name		initial_exh	
				Roughness from Material		steel	
				Imposed Wall Temperature	K	600	
				Link Name or Number		1-2-3	
		FlowSplitGeneral	exhmanturb-fs	Angle (Planar Configuration)		0-180-90	
				Characteristic Length_1	mm	21,85	
				Characteristic Length_2	mm	21,85	

				Characteristic Length_3	mm	21,85	
				Expansion Diameter_1	mm	78,99	
				Expansion Diameter_2	mm	78,99	
				Expansion Diameter_3	mm	110,586	
		PipeRectangle	turbine-in	Height at Inlet End	mm	15	
				Width at Inlet End	mm	25	
				Length	mm	20	
				Discretization Length	mm	40	
				Roughness from Material		steel	
				Initial State Name		initial_exh	
				Imposed Wall Temperature	K	600	
		OrificeConn	nocond	This orifice connection prevents conducti			
3. Turbocharger	3.1. Compressor	EndEnvironment	comp-inlet	Pressure (Absolute)	bar	1	
				Temperature	K	298	
				Composition		air	
		PipeRound	comp-in	Diameter at Inlet End	mm	70	65
				Diameter at Outlet End	mm	def	def
				Length	mm	250	100
				Discretization Length	mm	40	40
				Initial State Name		initial	intake_initial
				Rougness from Material		smooth_plastic	smooth_plastic
				Impossed wall Temperature		300	300
				Heat Transfer Multiplier		def	def
				Heat Input Rate		ign	ign
				Thermocouple Object		ign	ign
		Compressor	compressor	Rack Array		ign	
				Map Object or File		compressor_map	
	3.2. Turbine	Turbine	turbine	Rack Position		ign	
				Rack Array		ign	
				Map Object or File		turbine_map	
		PipeRound	turbine-out	Diameter at Inlet End	mm	55	
				Diameter at Outlet End	mm	def	
				Length	mm	320	
				Discretization Length	mm	55	
				Initial State Name		Post_turb_initial	Post_turb_initial
				Roughness from Material		steel	
				Wall Layer Properties Object		heat	
				Wall External Boundary Conditions Objec		heatWallLayer	
				Initial Wall Temperature	K	700	
		EndEnvironment	turbine-outlet	Pressure (Absolute)	bar	1	
				Temperature	K	298	
				Composition		air	
				Pressure Flag		standard(total)	
				Reversion Flow Composition		track	
	3.3. Connection	ShaftTurbo	shaft	Initial Speed	RPM	96000	96000
				Initial Speed for Case		RunSetupInitOption	
				Shaft Moment of Inertia	kg-m^2	0,0005	
				Friction Mechanical Efficiency	fraction	def	
				Inertia Multiplier		inertiamult	
4. Gas supply	4.1. Air inlet	PipeRound	venturi-in	Diameter at Inlet End	mm		65
				Diameter at Outlet End	mm		def
				Length	mm		100
				Discretization Length	mm		40
				Initial State Name			initial
				Rougness from Material			smooth_plastic
				Impossed wall Temperature			300
				Heat Transfer Multiplier			def
				Heat Input Rate			ign
				Thermocouple Object			ign
	4.3. Venturi	FlowSplitTRight	Venturi	Diameter	mm		65
				Length	mm		55
				Surface Area	mm^2		def
				Initial State Name			initial
				Surface Finish			
				Smooth			
				Imposed Wall Temperature	K		300
				Pressure (Absolute)	bar		1

	4.2. Gas inlet	EndEnvironment	Natural-gas-env	Temperature	K		298
				Composition			Natural_gas
		PipeRound	gas_inlet	Diameter at Inlet End	mm		30
				Diameter at Outlet End	mm		def
				Length	mm		500
				Discretization Length	mm		50
				Initial State Name			ambient
				Surface Finish			
				Smooth			
	4.3. Air-fuel ratio contorl	ControllerMassFlow	AFRController	Target Mass Flow Rate	kg/s		Actuated signal
				ThrottleConn or OrificeConn Part			AFRthrottle
				Display Performance Monitor			on
				Controller Version			V2016
		AFRthrottle	AFRThrottle	Reference Diameter	mm		25
				Throttle Angle			Actuated signal
		MathEquation	ichFuelFlowTar	Equation			AirFlow/AFR
				Airflow Wireless signal			2:bellmouth-5:79:79

Simulation reference objects

Type	GT-Power Template	Part Name	Properties	Unit	Sisudiesel 420 DWRIE model	Modified gas engine model
Flow	CompressorMap	compressor_map	Compressor Type		radial	
			External SAE File Name		ign	
			Create Pre-Process Plots?		on	
			Pre-processing Message Level		simple	
			Reference Pressure	bar	1	
			Reference Temperature	K	294	
			Reference Gas Constant	J/kg-K		
			Reference Ratio of Specific Heats			
			Wheel Diameter	mm		
			Flow Rate Input			
			*see Turbocharger_data_tables			
	EngCylCombDIWiebe	comb	Ignition Delay		3	
			Premixed Fraction		0,02	
			Tail Fraction		0,05	
			Premixed Duration		2	
			Main Duration		35	
			Tail Duration		40	
			Premixed Exponent		def	
			Main Exponent		def	
			Tail Exponent		def	
	EngCylCombSIWiebe	comb	Anchor Angle (def=50% burn)			8
			Duration (def=10% to 90%)			25
			Wiebe Exponent			2
			Knock Model Selection			standard-lastcycle
			Knock Model Object Name			knocking
	EngCylGeom	geom	Bore	mm	108	108
			Stroke	mm	120	120
			Connecting Rod Length	mm	208	208
			Compression Ratio		16,5	13
			TDC Clearance Height	mm	7,7	10
			Wrist Pin to Crank Offset	mm	1	1
			Stroke Convention		true-stroke	true-stroke
			TDC Angle Convention		piston-position	piston-position
	EngCyHeatTr	htr	Heat Transfer Model		WoschniGT	
			Overall Convection Multiplier		1	
			Head/Bore Area Ratio		1	
			Piston/Bore Area Ratio		1,2	
			Radiation Multiplier		ign	
			Convection Temperature Evaluation		hybrid	
			Low Speed Heat Transfer Enhancement for Wo		on	
	EngCylKnock	knocking	Knock Model			Kinetics-Fit-Natural-Gas
			End Gas Zones			Single-Zone
			Fuel Methane Number			81,9
	EngCylTWall	twall	Head Temperature	K	550	
			Piston Temperature	K	590	
			Cylinder Temperature	K	450	
	FluidInitialState	Intake_Initial	Pressure (Absolute)	bar		1
			Temperature	K		300
			Composition			Air_fuel
		initial	Pressure	bar	1	1
			Temperature	K	300	300
			Composition		air	air
		initial_exh	Pressure (Absolute)	bar	1,1	1,8
			Temperature	K	750	610
			Composition		exh_gas	air
			Pressure (Absolute)	bar		1

		Post_turb_initial	Temperature	K		300
			Composition			air
	FluidMixture	Air_fuel	air	%		96,3
			Natural_gas	%		3,7
	FluidMixtureBurned	exh_gas	air		95%	
			indolene-combust			
			diesel2-combust		5%	
	FluidMixtureCombined	Natural_gas	methane-vap			0,88
			ethane-vap			0,06
			propane-vap			0,06
	TurbineMapSAE	turbine_map	Turbine Map File		ign	
			Plots?		on	
			Pre-processing Message Level		simple	
			Reference Gas Constant	J/kg-K	289	
			Reference Ratio of Specific Heats		1,35	
			Maximum Pressure Ratio		4	
			Maximum Speed (Reduced)	RPM/K^0	3600	
			External SAE File Name		ign	
			Wheel Diameter (Affects Only Wheel	mm	def	
			*see Turbocharger_data_tables			
	WallThermalProperty	heat	Surface Emissivity		0,8	
			Layer Thickness	mm	3	
			Layer Material Object		Steel	
		inlet	Surface Emissivity		0,8	
			Layer Thickness	mm	3	
			Layer Material Object		StainlessSteel	
		InMan	Surface Emissivity		0,8	
			Layer Thickness	mm	3	
			Layer Material Object		Iron	
	WallThermalBoundary	inletWallLayer	External Convection Temperature	K	300	
			External Radiation Sink Temperature	K	300	
			External Convection Coefficient	W/(m^2-	15	
		InManWallLayer	External Convection Temperature	K	300	
			External Radiation Sink Temperature	K	300	
			External Convection Coefficient	W/(m^2-	15	
		heatWallLayer	External Convection Temperature	K	320	
			External Radiation Sink Temperature	K	320	
			External Convection Coefficient	W/(m^2-	15	
Mechanical	EngFrictionCF	friction	Constant part of FMEP	bar	0,4	
			Peak Cylinder Pressure Factor		0,005	
			Mean Piston Speed Factor	bar/(m/s	0,09	
			Mean Piston Speed Squared Factor	bar/(m/s	9,00E-04	
			Engine Speed Upon Entering Friction	RPM	def	
	ProfilePeriod	inertiamult	*see Turbocharger_data_tables			

Turbocharger data

Compressor Map

	RPM	kg/s		fraction
1	55984	0.15	1.75	0.67
2	55984	0.2113	1.703	0.737
3	55984	0.2769	1.669	0.763
4	55984	0.3333	1.608	0.735
5	55984	0.3948	1.494	0.639
6	73974	0.23	2.42	0.68
7	73974	0.3119	2.382	0.74
8	73974	0.3871	2.348	0.771
9	73974	0.4586	2.225	0.745
10	73974	0.5286	1.969	0.639
11	88485	0.36	3.21	0.69
12	88485	0.4388	3.191	0.746
13	88485	0.4869	3.152	0.758
14	88485	0.5468	2.963	0.731
15	88485	0.5975	2.536	0.635
16	102000	0.44	4.022	0.7
17	102000	0.52	4.018	0.709
18	102000	0.5455	3.967	0.712
19	102000	0.58	3.785	0.7
20	102000	0.63145	3.223	0.631

Turbine Map

	RPM/K^0,5	(kg/s)-K^0,5/kPa		Fraction
1	1821.9	0.027	1.22	0.68
2	1821.9	0.03	1.26	0.76
3	1821.9	0.032	1.30	0.79
4	1821.9	0.0349	1.35	0.806
5	1821.9	0.0352	1.38	0.785
6	2225.1	0.035	1.42	0.74
7	2225.1	0.037	1.47	0.76
8	2225.1	0.038	1.52	0.776
9	2225.1	0.04	1.57	0.784
10	2225.1	0.041	1.62	0.778
11	2567.4	0.0405	1.66	0.74
12	2567.4	0.041	1.71	0.76
13	2567.4	0.042	1.76	0.774
14	2567.4	0.043	1.81	0.78
15	2567.4	0.044	1.85	0.77
16	2863.6	0.0425	1.90	0.74
17	2863.6	0.043	1.95	0.76
18	2863.6	0.0435	2.00	0.775
19	2863.6	0.044	2.06	0.781
20	2863.6	0.0445	2.10	0.77
21	3133.6	0.0445	2.17	0.745
22	3133.6	0.045	2.26	0.76
23	3133.6	0.0452	2.35	0.776
24	3133.6	0.0454	2.44	0.782
25	3133.6	0.0456	2.52	0.77

Other data

Shaft initial speed	96000 RPM
Shaft moment of inertia	0.0005 kg-m^2

All the turbocharger data are those used in Gamma Technologies (2020) Tutorial 7.

GT-Power angle management

This section is a quick walkthrough about how GT-Power deals with valves openings according to crankshaft angles.

Template: *ValveCamConn*
Parts: *intvalve* and *exhvalve*

Cam Timing Angle*	Crank angle value at which the valve opening is maximal
Crank Angle	It means that when the piston is at TDC Firing, the crank angle is set to 0.
Theta = 0	At the tab *Lift*, at the column called *Angle array* the angle is set to 0 when the valve opening is maximal (Lift array).
Valve lash	Actuation space when the cam does not activate the valve – see figure below.

* see the last part of the section to know how to calculate that value

Valve lash

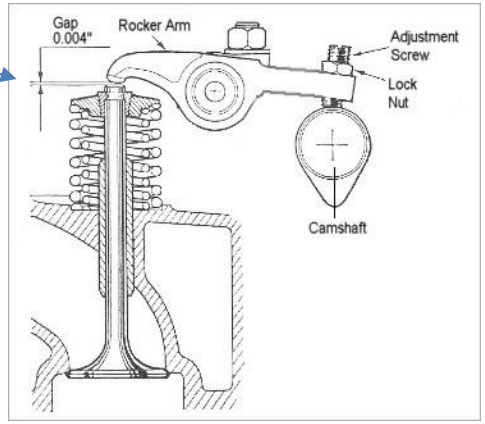

Adapted from ScooterFocus

	Manufacture		GT-Power	
Intvalve	Valve open (TDC) 0º	Valve close (BDC) 16º (after)	Valve open (TDC F) 360º	Valve close (TDC F) 556º
Exhvalve	Valve open (BDC) 39º (before)	Valve close (DC) 1º (after)	Valve open (TDC F) 141º	Valve close (TDC F) 361º

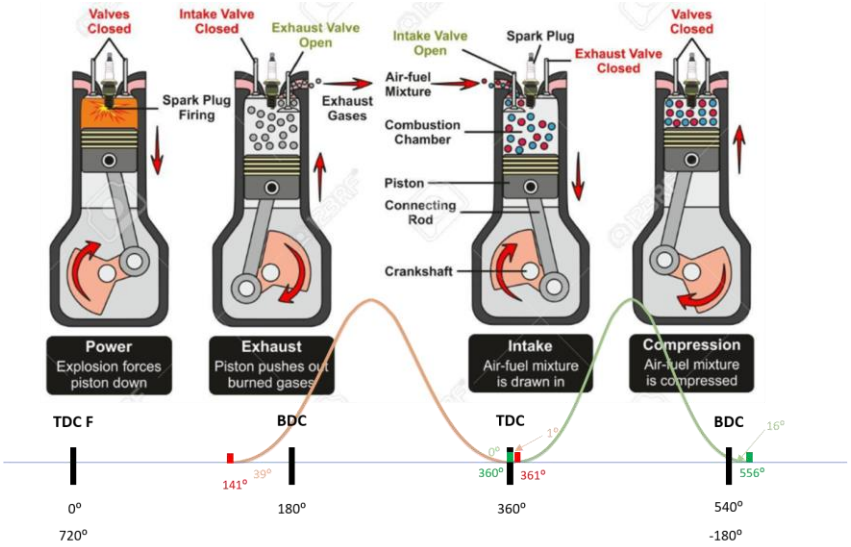

Adapted from 123RF

Calculation of Cam Timing Angle: mid-point between the *valve open* and the *valve close*.

Intvalve $\frac{556 + 360}{2} = 458^0$

Exhvalve $\frac{361 + 141}{2} = 251^0$

At these crank angle values, the valve is maximum opened (Lift Array) and the Angle Array must be 0

Appendix III. Sisudiesel 420 DWRIE performance

SISU Diesel

1998-05-27 J.KALLIO

TK9807

420 DWRIE ENGINE

ISO 8178 without fan

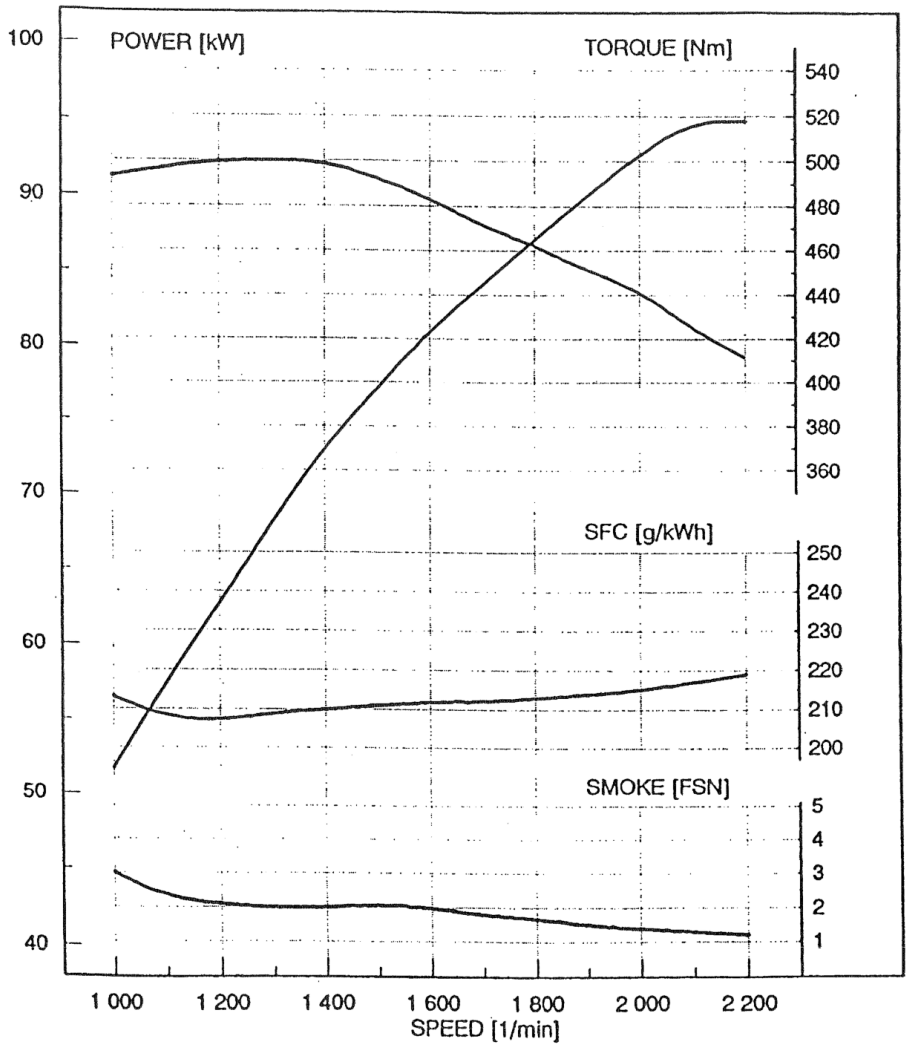

95 kW (129 hp) / 2200 rpm - 500 Nm / 1400 rpm - TBU 21 %
The power output is valid when the fuel density is 840 g/l at 15 C
and fuel temperature is 35 C.
Power ouput of a new engine is about 3% lower.
Fulfils EPA 96 and 97/68/EC exhaust emissions for non-road mobile machinery.

From the performance curves supplied by the manufacturer, some data points are obtained which are collected in the following table.

Engine speed (rpm)	Torque (Nm)	Power (kW)
1000	495	52
1100	499	57
1200	501	63
1300	501	68
1400	500	73
1500	492	77
1600	483	81
1700	471	84
1800	461	87
1900	451	90
2000	440	92
2100	423	94
2200	411	94.5

Appendix IV. GT-Power shared folder

A shared folder with all files used during the thesis is available at Novia University of Applied Sciences. There can be found all GT-Power files as well as Excel files with all the basic simulation parameters and extra calculations.